Imperfect drug penetration leads to spatial monotherapy and rapid evolution of multidrug resistance

Stefany Moreno-Gamez[a,b,1], Alison L. Hill[a,1], Daniel I. S. Rosenbloom[a,c], Dmitri A. Petrov[d], Martin A. Nowak[a], and Pleuni S. Pennings[d,e,f,2]

[a]Program for Evolutionary Dynamics, Department of Mathematics, Department of Organismic and Evolutionary Biology, Harvard University, Cambridge, MA 02138; [b]Theoretical Biology Group, Groningen Institute for Evolutionary Life Sciences, University of Groningen, Groningen, 9747 AG, The Netherlands; [c]Department of Biomedical Informatics, Columbia University Medical Center, New York, NY 10032; [d]Department of Biology, Stanford University, Stanford, CA 94305; [e]Department of Biology, San Francisco State University, San Francisco, CA 94132; and [f]Department of Organismic and Evolutionary Biology, Harvard University, Cambridge, MA 02138

Edited by Bruce R. Levin, Emory University, Atlanta, GA, and approved April 20, 2015 (received for review December 18, 2014)

Infections with rapidly evolving pathogens are often treated using combinations of drugs with different mechanisms of action. One of the major goal of combination therapy is to reduce the risk of drug resistance emerging during a patient's treatment. Although this strategy generally has significant benefits over monotherapy, it may also select for multidrug-resistant strains, particularly during long-term treatment for chronic infections. Infections with these strains present an important clinical and public health problem. Complicating this issue, for many antimicrobial treatment regimes, individual drugs have imperfect penetration throughout the body, so there may be regions where only one drug reaches an effective concentration. Here we propose that mismatched drug coverage can greatly speed up the evolution of multidrug resistance by allowing mutations to accumulate in a stepwise fashion. We develop a mathematical model of within-host pathogen evolution under spatially heterogeneous drug coverage and demonstrate that even very small single-drug compartments lead to dramatically higher resistance risk. We find that it is often better to use drug combinations with matched penetration profiles, although there may be a trade-off between preventing eventual treatment failure due to resistance in this way and temporarily reducing pathogen levels systemically. Our results show that drugs with the most extensive distribution are likely to be the most vulnerable to resistance. We conclude that optimal combination treatments should be designed to prevent this spatial effective monotherapy. These results are widely applicable to diverse microbial infections including viruses, bacteria, and parasites.

drug resistance | combination therapy | drug sanctuaries | spatial structure | pathogen evolution

Current standard-of-care treatment for many bacterial and viral infections involves combinations of two or more drugs with unique mechanisms of action. There are two main situations in which combination therapy significantly outperforms monotherapy (treatment with a single drug). First, in clinical scenarios where precise pathogen identification is not possible before treatment begins ("empirical therapy"), or when infections are suspected to be polymicrobial, treating with multiple drugs increases the chances of targeting the virulent organism. Second, even when infections are caused by a single, precisely identified microbe, combination therapy reduces the risk of developing drug resistance. This reduced risk is believed to follow from the fact that multiple mutations are generally needed to enable pathogen growth when multiple drugs are present. In addition, the use of multiple drugs may reduce the residual population size and thus further reduce the rate of evolution of resistance. Preventing the evolution of resistance is particularly relevant to infections caused by rapidly evolving pathogens and to persistent infections that can be controlled but not cured, for which there may be a high risk of drug resistance evolving during the course of a single patient's treatment. Despite widespread use of combination therapy, drug resistance remains a serious concern for many infections in this category, such as the human immunodeficiency virus (HIV), hepatitis B virus (HBV), hepatitis C virus (HCV), *Mycobacterium tuberculosis* (TB), and other chronic bacterial infections (1–5), as well as for certain cancers (6, 7). Understanding the factors that facilitate the evolution of multidrug resistance is therefore a research priority.

Combination therapy can be compromised by treatment regimes that allow resistance mutations to different drugs to be acquired progressively (i.e., in stepwise fashion) rather than concurrently. This can occur when only one drug of the combination is active during certain time periods. For example, starting patients on a single drug before adding a second drug promotes the evolution of multidrug resistance (8–11). A similar effect is seen for studies that rotate antibiotics (12–14). Even if drugs are given simultaneously but have different in vivo half-lives (15–17) or postantibiotic effects (18), periods of "effective monotherapy" with the longer-lived drug can occur, which may favor resistance evolution.

Significance

The evolution of drug resistance is a major health threat. In chronic infections with rapidly mutating pathogens—including HIV, tuberculosis, and hepatitis B and C viruses—multidrug resistance can cause even aggressive combination drug treatment to fail. Oftentimes, individual drugs within a combination do not penetrate equally to all infected regions of the body. Here we present a mathematical model suggesting that this imperfect penetration can dramatically increase the chance of treatment failure by creating regions where only one drug from a combination reaches a therapeutic concentration. The resulting single-drug compartments allow the pathogen to evolve resistance to each drug sequentially, rapidly causing multidrug resistance. More broadly, our model provides a quantitative framework for reasoning about trade-offs between aggressive and moderate drug therapies.

Author contributions: S.M.-G., A.L.H., D.I.S.R., and P.S.P. designed research; S.M.-G., A.L.H., D.I.S.R., and P.S.P. performed research; S.M.-G., A.L.H., D.I.S.R., D.A.P., M.A.N., and P.S.P. contributed new reagents/analytic tools; and S.M.-G., A.L.H., D.I.S.R., D.A.P., M.A.N., and P.S.P. wrote the paper.

The authors declare no conflict of interest.

This article is a PNAS Direct Submission.

Freely available online through the PNAS open access option.

[1]S.M.-G. and A.L.H. contributed equally to this work.

[2]To whom correspondence should be addressed. Email: pennings@sfsu.edu.

This article contains supporting information online at www.pnas.org/lookup/suppl/doi:10.1073/pnas.1424184112/-/DCSupplemental.

HIV and TB are pathogens for which evolution of drug resistance is well studied. Surprisingly, it has been found that stepwise evolution of drug resistance is common in treated HIV- (19–21) and TB-infected individuals (18). It is unclear whether periods of effective monotherapy can explain this observation.

Whereas many recent studies have focused on the potential impact of different half-lives between drugs, much less is known about how the spatial distribution of drugs influences the evolution of multidrug resistance during combination therapy. Many treatments may involve mismatched drug penetrability—that is, there may be regions of the body where only a subset of drugs within a combination reaches a therapeutic level (22, 23). For example, many anti-HIV drugs have been observed at subclinical concentrations in the central nervous system, the genital tract, and some lymph tissue (24–26). Low concentrations in these body compartments, even when plasma concentrations are high, may allow viral replication and selection of resistance mutations (22, 27, 28), which may eventually migrate to the blood and lead to treatment failure (29). In another example, poor antibiotic penetration within biofilms (30) or certain body tissues (31) during treatment for *Staphylococcus aureus* infections is again associated with resistance evolution. Some medical practitioners recommend that this problem be addressed by pairing drugs with high efficacy but low penetration with other drugs of higher penetration, so that total drug coverage in the body increases (31). However, this is likely a risky strategy. We hypothesize that combination therapy with drugs that have different penetration profiles will generally be more vulnerable to resistance, as it promotes situations of effective monotherapy that may allow a migrating pathogen lineage to acquire resistance mutations in a stepwise manner.

Previous work on the effect of drug penetration on drug resistance has mainly focused on monotherapy. A mathematical model of viral infections showed that the window of drug concentrations where resistance mutations can arise and fix is greatly increased if there is a "drug-protected compartment" or "drug sanctuary"—a place where the drug level is not high enough to prevent virus replication (32). More recent theoretical work has explored the role of concentration gradients in the evolution of antibiotic resistance. This work demonstrated that when multiple mutations are needed for resistance to a single drug, either a continuous concentration gradient (33) or discrete microenvironments with differing concentrations (34) can speed up the rate of evolution. Experiments in microfluidic chambers where mobile bacteria grow in the presence of a spatial drug concentration gradient have confirmed that adaptation is accelerated (35). These results are surprisingly similar to studies that create temporal gradients in drug concentrations (36).

A few detailed simulation studies have examined resistance evolution during combination antibiotic therapy and included sources of heterogeneity in drug efficacy (37–39). These models used experimentally determined pharmacodynamic parameters and included subpopulations of slow-growing persister bacteria that may be less sensitive to one or all antibiotics in a combination. Although these studies did not specifically focus on quantifying the role of effective monotherapy due to mismatched drug distributions, they strongly suggest that it may play a role in multidrug resistance.

In this paper, we examine the general role that drug penetration plays in evolution of resistance during combination therapy—thereby addressing a broad range of effective drug treatments. Specifically, we use a mathematical modeling strategy to show how the existence of anatomical compartments where only single drugs are present can drastically change the rate at which multidrug resistance emerges and leads to systemic infection despite treatment. Among several pharmacologic and genetic determinants of resistance, we find that the size of single-drug compartments is key. A simple mathematical expression describes the critical size of single-drug compartments above which drug resistance emerges at an elevated rate, due to stepwise accumulation of mutations. In addition, we discover that combination therapy strategies face a general trade-off between suppressing microbial growth throughout the entire body and preventing eventual emergence of multidrug resistance. This trade-off implies, perhaps counterintuitively, that it may be rational to allow low-level microbial growth restricted to a small compartment where no drugs penetrate, to avoid regions of mismatched drug penetration—and increased risk of resistance emerging in the entire body. We discuss implications of this work for designing optimal drug combinations to prevent spatial effective monotherapy. Finally, we use our theory to explain why stepwise evolution of resistance may occur during effective combination therapy, as is sometimes seen clinically.

Model

Our goal is to understand the role of drug penetration in the evolution of multidrug resistance. We consider an individual patient's body to be divided into discrete and interconnected compartments where each drug either effectively suppresses pathogen growth or is completely absent (Fig. 1). We model microbial dynamics in this environment, including growth, mutation, competition between strains, and migration between compartments. For simplicity, we focus on the case of two drugs only, although extensions to combinations of three or more drugs are straightforward.

To describe population dynamics of the pathogen in this scenario, we use a viral dynamics model (40) (*SI Appendix*) that tracks infected and uninfected cells. We analyze the model, using a fully stochastic simulation (*SI Appendix*), and derive approximate analytic formulas to describe the dominant processes. Other ways of modeling pathogen growth with limited resources, such as the logistic model, could be used instead and we expect this would have little influence on the results. In this model, pathogen fitness can be measured in terms of the basic reproductive ratio R_0, the number of new infections generated by a single infected cell before it dies, when target cells are in excess. A strain can lead to a sustainable infection in a compartment only if $R_0 > 1$ (i.e., growth is positive). When this occurs, the pathogen population can reach an equilibrium level that we refer to as the carrying capacity (K).

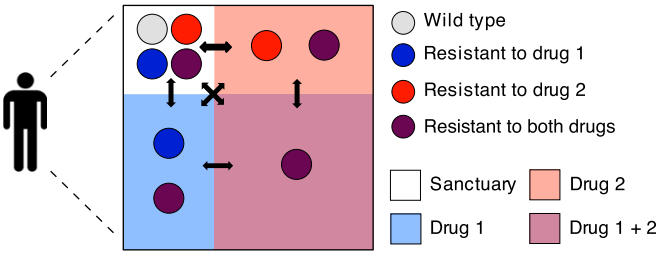

Fig. 1. Compartment model for combination therapy with two drugs. The box represents a patient's body and the red and blue shaded areas indicate the presence of drug 1 and drug 2, respectively. Mismatched drug penetration creates regions in the body where only one drug from the combination is present. We refer to these regions as single-drug compartments. Colored circles represent the pathogen genotypes: wild type (light gray), mutant resistant to drug 1 (blue), mutant resistant to drug 2 (red), and double-drug-resistant mutant (purple). In the sanctuary all of the pathogen genotypes can grow because none of the drugs is present. In the single-drug compartments only pathogens carrying a resistance mutation against the active drug can grow; that is, each drug alone suppresses pathogen growth. Finally, in the double-drug compartment only the double-drug-resistant mutant can grow. All of the compartments are connected by migration as indicated by the black arrows. Treatment failure occurs when the double-drug compartment, which always composes the majority of the body, is colonized by the double mutant. Note that we do not always require that both single-drug compartments exist, and the compartment sizes may not follow this particular geometric relationship.

We consider at most four compartments within a single patient (Fig. 1): one compartment where no drugs are present (the sanctuary), two compartments where only one of the drugs is present (single-drug compartments 1 and 2), and one compartment where both drugs are present (the double-drug compartment, which we always take to be by far the largest compartment). The pathogen population within each compartment is assumed to be well mixed and follows the viral dynamics model. The size of each compartment j is given by the number of target cells N_j that it contains when infection is absent. The carrying capacity K_{ij} of pathogen strain i infecting compartment j increases monotonically with pathogen fitness (R_0^{ij}) and is always less than the compartment size ($K_{ij} < N_j$ for all i), assuming that the death rate of infected cells exceeds that of uninfected cells. In the absence of mutation or migration, there is competitive exclusion between strains within a compartment, and the strain with the highest fitness goes to fixation. With migration or mutation, multiple strains may coexist within a compartment, although the locally suboptimal strains generally occur at much lower frequencies.

The four compartments are connected by migration of pathogens (but not drugs), and every strain in the body migrates from compartment j to compartment k at a rate m_{jk} per time. We use a simple and biologically realistic migration scheme in which each pathogen migrates out of its home compartment at the same rate m. Migrants from a given compartment are then distributed into all four compartments (including the one they came from) proportionally to the compartment sizes, so that larger compartments get more migrants.

A single mutation is needed for resistance to each drug. Mutations conferring resistance to drug i occur at a rate μ_i (and can revert at the same rate). Resistance to two drugs requires that both mutations occur, and we do not allow recombination or any other form of lateral gene transfer to break linkage between the two mutations. We design our fitness landscape so that four assumptions are met: (*i*) Each drug alone suppresses pathogen growth, (*ii*) a wild-type pathogen in the sanctuary has the highest possible fitness, (*iii*) a doubly resistant pathogen is always viable, and (*iv*) in the single-drug compartments, the strain with resistance only to the drug present is the fittest. Formally, if a strain is not resistant to a drug i present in the compartment where it resides, its fitness is reduced by a factor of $1-\epsilon_i$, where $\epsilon_i \in [0,1]$ is the drug efficacy. Resistance mutations come with a fitness cost $s_i \in [0,1]$. The fitness of resistant strains is completely unaffected by the presence of the drug. The fitness values for each genotype in each compartment, relative to that of a wild-type strain in the sanctuary (R_{WT}), are shown in Table 1. To satisfy condition *i*, we constrain $R_{WT}(1-\epsilon_i) < 1$, and to meet condition *iii*, we require $R_{WT}(1-s_1)(1-s_2) > 1$. At the start of treatment, we suppose the wild-type pathogen to be present in all compartments; we first focus on the case without preexisting resistance mutations and later consider how preexisting resistance alters results.

We apply this model to a physiologic scenario where the double-drug compartment occupies the vast majority of the body and where isolated infections within the small sanctuary or single-drug sites are not life threatening on their own. Therefore, treatment failure is said to occur when the multidrug-resistant mutant colonizes the double-drug compartment. We define colonization as a pathogen load high enough such that the probability of chance extinction is negligible. We investigate how the presence and size of single-drug compartments—created by combinations of drugs with mismatched penetration profiles—determine two clinical outcomes: the rate at which treatment failure occurs and the evolutionary path by which the multidrug-resistant mutant emerges. Under the direct evolutionary path, multiple-resistance mutations are acquired near simultaneously [this is sometimes referred to as "stochastic tunneling" (41, 42)]; under stepwise evolution, a single-drug compartment is colonized with a single-resistant strain before the emergence of multidrug resistance.

Results

Mismatched Drug Penetration Can Speed Up Emergence of Resistance. Using parameter values appropriate for HIV treatment (*SI Appendix*), we simulate pathogen evolution according to the model described above. For simplicity, we first consider the presence of only one single-drug compartment (containing drug 1). The probability of treatment failure via double-drug resistance after 1 year (Fig. 2*A*) or 10 years (Fig. 2*B*) increases dramatically with the size of the single-drug compartment, even when this region is two to three orders of magnitude smaller than the area covered by both drugs. This demonstrates that imperfect drug penetration can be highly detrimental to treatment outcomes.

Mismatched drug penetration hastens the emergence of multidrug resistance by allowing for stepwise evolution (Fig. 2 *C* and *D*). Specifically, single-resistant mutants can evade competition with wild-type strains by migrating to the single-drug compartment, which serves as a platform from which resistance to the second drug may evolve (Fig. 2*D*). When drugs have identical penetration, there are only two compartments—the sanctuary and the double-drug compartment. In typical simulations (Fig. 2*C*), single-resistant mutants arising in the sanctuary are driven recurrently to extinction by the fitter wild type. As a result, the only way that double-drug resistance can emerge is by appearance of both mutations nearly simultaneously, enabling successful migration to the double-drug compartment (direct evolution). This slow process increases time to treatment failure.

Consistent with the above explanation, the prevalence of failure by direct evolution depends weakly on single-drug compartment size, only decreasing slightly with compartment size as the competing stepwise path occurs first (Fig. 2 *A* and *B*). Failure by stepwise evolution, however, increases substantially with the size of the single-drug compartment, and it is the dominant path if the single-drug compartment exceeds a critical size, investigated below.

Stepwise vs. Direct Evolution. Using a simplified model of colonization of each compartment, we can approximate the critical single-drug compartment size above which stepwise evolution becomes the dominant process. Specifically, we approximate

Table 1. The fitness of each pathogen strain in each compartment relative to the fitness of the wild-type strain in the absence of the drug (R_{WT})

	Sanctuary	SDC 1	SDC 2	DDC
Wild type	1	$1-\epsilon_1$	$1-\epsilon_2$	$(1-\epsilon_1)(1-\epsilon_2)$
Single mutant 1	$1-s_1$	$1-s_1$	$(1-s_1)(1-\epsilon_2)$	$(1-s_1)(1-\epsilon_2)$
Single mutant 2	$1-s_2$	$(1-s_2)(1-\epsilon_1)$	$1-s_2$	$(1-s_2)(1-\epsilon_1)$
Double mutant	$(1-s_1)(1-s_2)$	$(1-s_1)(1-s_2)$	$(1-s_1)(1-s_2)$	$(1-s_1)(1-s_2)$

The efficacy of drug i is ϵ_i and the fitness cost of resistance to drug i is s_i. DDC, double-drug compartment; SDC, single-drug compartment.

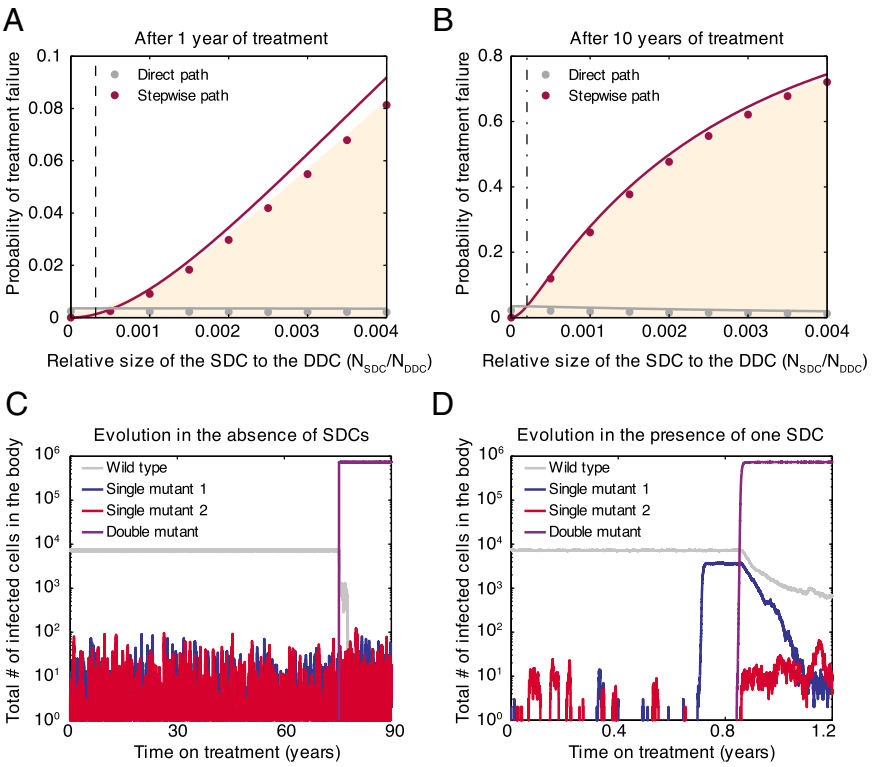

Fig. 2. Resistance evolution in the presence of a single-drug compartment. Even a small single-drug compartment can considerably speed up the evolution of double-drug resistance. (*A* and *B*) The shaded area gives the fraction of simulated patients that failed treatment after 1 year or 10 years as a function of the size of the single-drug compartment containing drug 1 (SDC1) relative to the size of the double-drug compartment (DDC). We further indicate whether treatment failure occurred via direct (gray circles) or stepwise (pink circles) evolution. Solid lines are analytic calculations (*SI Appendix*, sections 5 and 6). The vertical dotted lines are further simplified, closed-form analytical expressions for the point where the stepwise path to resistance becomes more important than the direct path (*SI Appendix*, sections 4.2 and 7). (*C* and *D*) Evolution of drug resistance over time for a simulated patient in the absence (*C*) or presence (*D*) of SDC1. When there are no single-drug compartments, mutants resistant to drug 1 go to extinction recurrently by competition with the wild type in the sanctuary, whereas in the presence of SDC1, mutants resistant to drug 1 can escape competition and establish a continuous population (blue line) from which a doubly resistant strain can evolve (purple). Parameters: $R_{WT} = 4$, $\epsilon_1 = 0.99$, $\epsilon_2 = 0.99$, $d_y = 1\ d^{-1}$, $d_x = 0.1\ d^{-1}$, $m = 0.1\ d^{-1}$, $s_1 = 0.05$, $s_2 = 0.05$, $\mu_1 = 10^{-5}$, $\mu_2 = 10^{-5}$, $N_{SAN} = 10^5$ cells, $N_{SDC2} = 0$ cells, $N_{DDC} = 10^7$ cells. N_{SDC1} changes along the *x* axis for *A* and *B* and for each value of N_{SDC1} treatment has failed in at least 2,000 simulated patients. $N_{SDC1} = 0$ for *C* and $N_{SDC1} = 5 \times 10^4$ cells for *D*.

the colonization process by transitions between discrete states of the population, where each state is described by the presence or absence of each strain in each compartment. For brevity, we assume that the mutation rate and fitness cost are the same for both mutational steps and that there is only one single-drug compartment. In state 0, only the sanctuary is colonized (by the wild-type strain); in state 1, the single-drug compartment is also colonized (by the single-resistant mutant); and state 2 is the end state where the double-drug compartment is colonized (by the double-resistant strain). Rates of treatment failure can be computed exactly in this simplified model (*SI Appendix*, sections 4–6), which provides an excellent approximation to the full stochastic simulation (Fig. 2 *A* and *B*).

Using this model, we can obtain simple approximate expressions for the size of the single-drug compartment (SDC) where the stepwise path starts to overtake the direct path (detailed in *SI Appendix*, section 7). The SDC becomes colonized (transition from state 0 to state 1) by one of two events. Either a mutation occurs within the sanctuary, and then that strain migrates to the SDC, or a wild-type strain migrates from the sanctuary to the SDC, where it manages to replicate and mutate despite the presence of the drug. In both cases the mutant must escape extinction to establish an infection in the SDC. In the limit where mutation cost is small ($s \ll 1$) but drug efficacy is high ($\epsilon \approx 1$), mutation typically precedes migration, and the rate of invasion of the single-drug compartment is approximately

$$r_{01} \approx \frac{\mu}{s} K_{SAN}^{WT} \left(m \frac{N_{SDC}}{N_{TOT}} \right) \left(1 - \frac{1}{R_{WT}(1-s)} \right).$$

Here $(\mu/s)K_{SAN}^{WT}$ is the number of single mutants in the sanctuary ("SAN," at mutation–selection equilibrium), $m(N_{SDC}/N_{TOT})$ is the migration rate to the single-drug compartment, and $(1 - 1/R_{WT}(1-s))$ is the establishment probability of a resistant mutant in the single-drug compartment (see *SI Appendix* for full derivation with respect to the viral dynamics model). If invasion is successful, we assume that the population in the newly invaded compartment reaches its carrying capacity (K_{SDC}^1) instantaneously. Doing so relies on a separation of timescales between the slow processes of mutation and migration and the faster process of growth to equilibrium.

Similarly, once the single-drug compartment is colonized, the double-drug compartment (DDC) can be invaded. Again, the mutation–migration path is most likely, with rate approximately

$$r_{12} \approx \frac{\mu}{s} K_{SDC}^1 \left(m \frac{N_{DDC}}{N_{TOT}} \right) \left(1 - \frac{1}{R_{WT}(1-s)^2} \right).$$

The double-drug compartment can also be invaded directly from the sanctuary. There are three paths by which this can happen, depending on whether none, one, or both of the necessary mutational steps occur before migration. By the same logic as

above, the mutation–mutation–migration path is most likely, and the rate is approximately

$$r_{02} \approx \frac{\mu^2}{s^2} K_{\mathrm{SAN}}^{\mathrm{WT}} \left(m \frac{N_{\mathrm{DDC}}}{N_{\mathrm{TOT}}} \right) \left(1 - \frac{1}{R_{\mathrm{WT}}(1-s)^2} \right).$$

In the scenario under consideration, the mutation rate is much smaller than the cost of mutations ($\mu/s \ll 1$) so that $\mu^2/s^2 \ll \mu/s$. We also assume that both drugs penetrate in a large part of the body so that the double-drug compartment is always much larger than the single-drug compartment ($N_{\mathrm{SDC}} \ll N_{\mathrm{DDC}}$). It is therefore likely that $r_{01} \ll r_{12}$ and $r_{02} \ll r_{12}$. Using these expressions, we can determine the overall rate at which the DDC becomes colonized via the SDC (stepwise evolution) and compare it to the rate of direct evolution.

First, we consider treatment outcomes when a short enough time (t) has passed so that drug resistance is rare and all steps are rate limited ($r_{01}t \ll 1$, $r_{12}t \ll 1$, $r_{02}t \ll 1$). In this regime, the minimum size of the SDC at which stepwise evolution outpaces the direct path (lines cross in Fig. 2 *A* and *B*) increases with the pathogen virulence ($\approx K_i^1/N_i$), but decreases with the migration rate (m) and (weakly) with the fitness of the single mutant ($R_{\mathrm{WT}}(1-s)$). It also decreases with the time of observation (t) because the stepwise path requires two steps, so that for very small t, the SDC needs to be larger for it to be possible that both steps are completed. This approximation (*SI Appendix*, section 7, *Approximation 1*) describes the cross point after 1 year of treatment well (Fig. 2*A*).

Alternatively, if the treatment time is long enough so that most individuals who developed single-drug resistance progressed to treatment failure ($r_{12}t > 1$), but the other (slower) steps remain rate limiting, then a simpler and more intuitive result emerges: The stepwise path is more important than the direct path if

$$\frac{N_{\mathrm{SDC}}}{N_{\mathrm{DDC}}} > \frac{\mu}{s}.$$

The single-drug compartment therefore plays an important role if its size, relative to that of the double-drug compartment, is at least equal to the mutation-to-cost ratio. Intuitively, if mutations are rare and costly, then double mutants occur infrequently and the stepwise path to multidrug resistance is relatively more important. Even if mutations are rather common (say, $\mu = 10^{-5}$) and not very costly ($s = 10^{-3}$), the stepwise path is still dominant if the single-drug compartment is at least 1/100th the size of the double-drug compartment. For the parameters used in the figures, this approximation describes the cross point after 10 years of treatment well (Fig. 2*B*).

Trade-Off Between Halting Pathogen Growth and Preventing Resistance. The choice of antimicrobial therapy generally presents a trade-off between maximizing clinical efficacy and minimizing the chance that drug resistance emerges (43). The spatial setting introduces new dimensions to this trade-off. In this setting, minimizing the size of single-drug compartments can impede the stepwise evolution of resistance. Pursuing this goal, however, involves choosing drugs that penetrate the same anatomical regions, potentially reducing the portion of the body that receives any drug at all. The physician therefore may sometimes be faced with a trade-off: to halt wild-type growth immediately (smaller sanctuary) or to prevent stepwise evolution of resistance (smaller single-drug compartments).

To investigate this trade-off, we vary single-drug compartment size relative to the sanctuary, keeping double-drug compartment and total system size constant (Fig. 3). We do this analysis imagining that one drug of the combination is fixed, and another can be chosen that has either equal or greater penetration.

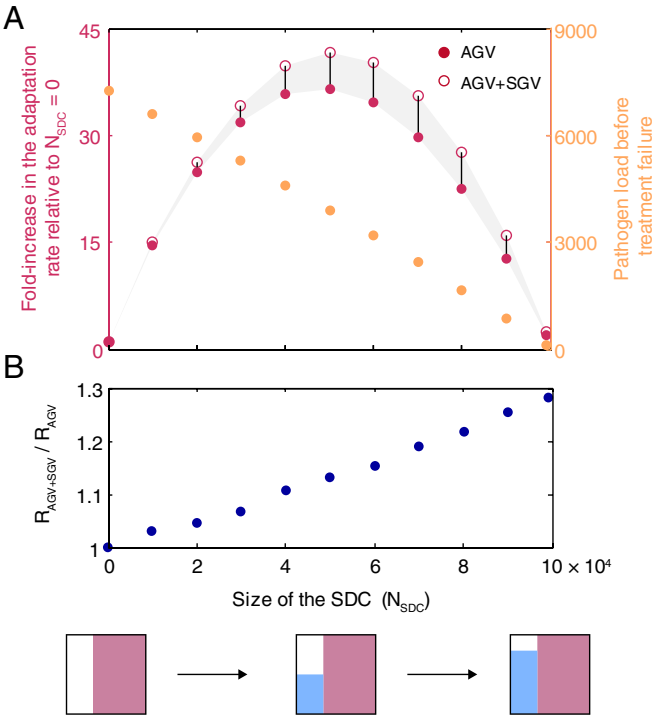

Fig. 3. Trade-off between total drug coverage and the presence of single-drug compartments. (*A*) The adaptation rate (purple circles, left *y* axis) and time-averaged infection size (orange circles, right *y* axis) are plotted as a function of the size of the single-drug compartment with drug 1 (N_{SDC1}), assuming that the sum of the sizes of the sanctuary (N_{SAN}) and SDC1 is constant. Diagrams below the *x* axis illustrate the changes in compartment sizes, following the style of Fig. 1. The adaptation rate is defined as the inverse of the mean time to treatment failure and is plotted relative to the rate when $N_{\mathrm{SDC1}} = 0$. We show adaptation rate only from acquired genetic variation (solid circles) and from both acquired and standing genetic variation (i.e., preexisting resistance, open circles); the difference is shown by the gray area and the vertical lines. The infection size is calculated as the mean of the time-averaged number of infected cells in all compartments before treatment failure occurs. Increasing the size of the single-drug compartment provides better control of the infection before treatment fails, but strongly favors resistance evolution if the reduction of the sanctuary is not large enough. (*B*) Ratio of the rate of adaptation from standing and acquired genetic variation ($R_{\mathrm{SGV+\,AGV}}$) to the rate of adaptation only from acquired genetic variation (R_{AGV}). The relative contribution of standing genetic variation to treatment failure increases with the size of the SDC. Parameters: $R_{\mathrm{WT}} = 4$, $\epsilon_1 = 0.99$, $\epsilon_2 = 0.99$, $d_y = 1\ \mathrm{d}^{-1}$, $d_x = 0.1\ \mathrm{d}^{-1}$, $m = 0.1\ \mathrm{d}^{-1}$, $s_1 = 0.05$, $s_2 = 0.05$, $\mu_1 = 10^{-5}$, $\mu_2 = 10^{-5}$, $N_{\mathrm{SAN}} = 10^5 - N_{\mathrm{SDC1}}$, $N_{\mathrm{SDC2}} = 0$ cells, $N_{\mathrm{DDC}} = 10^7$ cells. Each point is an average over at least 30,000 simulated patients.

Consistent with the above findings, the rate of treatment failure by double-drug resistance increases dramatically as single-drug compartment size increases from zero. At the same time, however, the sanctuary shrinks from its maximum size, reducing total pathogen load in the body before failure.

The trend in treatment failure reverses, however, as the sanctuary is further reduced (right half of Fig. 3*A*). Even when stepwise evolution is still the dominant mode of treatment failure, a small sanctuary limits the rate at which single mutations are generated and therefore decreases the overall rate of emergence of multidrug resistance. In the complete absence of a sanctuary, treatment failure can occur only if preexisting resistance is selected or if resistance is generated very quickly after treatment starts. Because these events are not guaranteed, cure becomes a possible outcome (*SI Appendix*, Fig. S1) and the rate of resistance evolution is dramatically reduced. The rate of treatment failure is greatest when the sanctuary and single-drug compartment are

similar in size, highlighting the fact that stepwise evolution is driven by interaction between a sanctuary and single-drug compartments.

These findings suggest that eliminating all sanctuary sites should be a primary goal (moving toward far right in Fig. 3*A*), because this reduces pathogen load and the risk that resistance evolves. If this is not feasible (for example, if the pathogen has a latent phase not targeted by treatment), then preventing any zones of single-drug coverage should take precedence to keep the rate of evolution of drug resistance as low as possible (moving toward far left in Fig. 3*A*).

Accounting for Preexisting Mutations. To focus clearly on the processes by which resistance is acquired during combination therapy, we have so far ignored the contribution of preexisting mutants (known in the population genetics literature as "standing genetic variation"). To instead include this factor, we simulate the model for a period before the introduction of treatment, allowing both single- and double-resistant mutants to occur along with the wild-type strain in each compartment. Previous work has focused extensively on comparing the relative roles of preexisting and acquired resistance in viral dynamics models (21, 44–46), and here we simply summarize the trends in our model.

The addition of preexisting resistance acts to increase the overall rate of treatment failure, and this increase is more prominent for certain parameter values and for smaller treatment times (compare *SI Appendix*, Fig. S2*A* with Fig. 2*A*). However, the inclusion of preexisting resistance does not affect any of the general trends, such as the dominant path to resistance (*SI Appendix*, Fig. S2) or the trade-off between the size of the sanctuary and the single-drug compartment (Fig. 3). Importantly, the role of preexisting resistance—defined as the percentage of failures attributable to standing genetic variation—increases dramatically with single-drug compartment size (Fig. 3*B*). Therefore, the presence of compartments where only single drugs penetrate can increase the rate of treatment failure both by making it quicker to acquire multiple-resistance mutations and by selecting for preexisting single-drug-resistant mutants.

Preexisting mutations are particularly relevant for curable infections, as opposed to chronic ones. In such infections, either a sanctuary zone does not exist or it is small enough to be eradicated by immune responses. As treatment duration is limited, treatment failure can occur only if there are preexisting resistance mutations or if the pathogen acquires resistance shortly after treatment starts. In this limit, the dynamics are a classic "race to rescue" described by Orr and Unckless (47), which results in either cure or treatment failure. We find that zones of mismatched penetration reduce the probability of curing the infection (*SI Appendix*, Fig. S1) by selecting for single-drug-resistant mutations that would otherwise become extinct under combination therapy. In a scenario where sanctuary regions exist initially but eventually decay (for example, if they are caused by long-lived persister cells), we expect that mismatched drug penetration will both decrease the probability of cure and decrease the time to resistance in those patients in whom cure is not achieved.

Order of Mutations. Because pharmacological factors determining penetration of anatomical compartments vary widely among drugs (23, 25, 30, 48), we generally expect that each drug in a combination has its own single-drug compartment. In this general case, we can ask, To which drug does the pathogen become resistant first? More precisely, if stepwise evolution occurs, is it likely to be through the path SAN → SDC1 → DDC or SAN → SDC2 → DDC? Examining the rate of each path as a function of the size of each single-drug compartment (Fig. 4*A*) shows that resistance is more likely to emerge first to the drug with the highest coverage (and therefore largest SDC) and that the odds of resistance occurring to one drug before another are proportional to the ratio of the corresponding SDCs over a large parameter range.

Moreover, the mutation rates and costs associated with resistance to each drug may differ, also influencing the likelihood of a particular path to resistance. Resistance is more likely to emerge first for the drug associated with the highest mutation rate (Fig. 4*B*) and lowest fitness cost (Fig. 4*C*), with the relative rates again being approximated by the ratios of the parameters. Drug efficacy may also vary, although in the regime where each drug individually suppresses wild-type pathogen growth ($R_{WT}(1-\epsilon) \ll 1$) and the cost of mutations is not too high ($s < \epsilon$), drug efficacy barely influences the order in which resistance mutations are acquired (*SI Appendix*, Fig. S3).

Discussion

Antimicrobial drugs fail to reach effective concentrations in many tissues and body organs, allowing pathogen replication and potential evolution of resistance (26, 28, 31, 48, 49). We studied the role of imperfect drug penetration in the development of drug

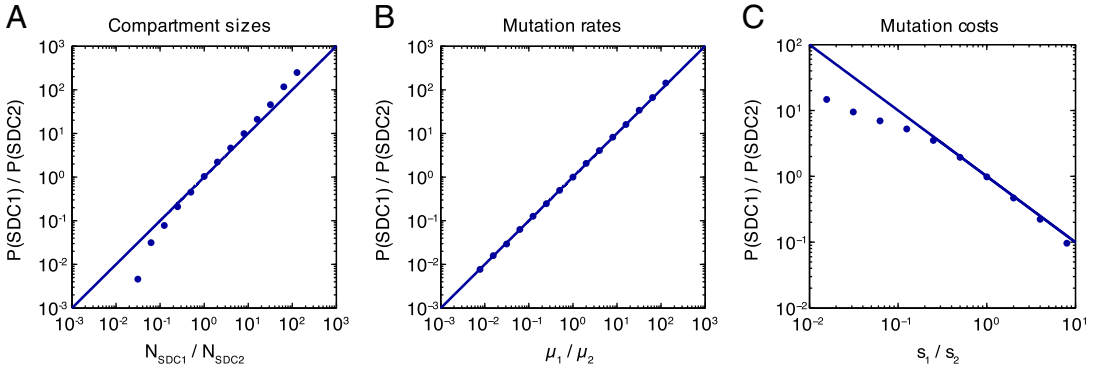

Fig. 4. Stepwise resistance evolution in the presence of two single-drug compartments. (*A*–*C*) Fraction of simulated patients that failed via the path where the single-drug compartment with drug 1 is colonized before treatment failure (P(SDC1): SAN → SDC1 → DDC) relative to the fraction that failed via the path where the single-drug compartment with drug 2 is colonized before (P(SDC2): SAN → SDC2 → DDC) as a function of (*A*) compartment sizes, (*B*) mutation rates, and (*C*) mutation costs. (*A*) The *x* axis corresponds to the ratio of the size of the single-drug compartment with drug 1 (N_{SDC1}) to the size of the single-drug compartment with drug 2 (N_{SDC2}). (*B*) The *x* axis corresponds to the ratio of the mutation rate for resistance to drug 1 (μ_1) to the mutation rate for resistance to drug 2 (μ_2). (*C*) The *x* axis corresponds to the ratio of the cost of a resistance mutation to drug 1 (s_1) to the cost of a resistance mutation to drug 2 (s_2). Simulation results (circles) are overlaid with the lines $y = x$ (*A* and *B*) or $y = 1/x$ (*C*). Parameters: $R_{WT} = 4$, $\epsilon_1 = 0.99$, $\epsilon_2 = 0.99$, $d_y = 1\ d^{-1}$, $d_x = 0.1\ d^{-1}$, $m = 0.1\ d^{-1}$, $s_1 = 0.05$, $s_2 = 0.05$, $\mu_1 = 10^{-5}$, $\mu_2 = 10^{-5}$, $N_{SAN} = 10^5$ cells, $N_{SDC1} = 10^4$ cells, $N_{SDC2} = 10^4$ cells, $N_{DDC} = 10^7$ cells. N_{SDC1} changes along the *x* axis (*A*), μ_1 changes along the *x* axis (*B*), and s_1 changes along the *x* axis (*C*). The total number of simulated patients for each point is at least 6,000.

resistance during combination therapy, using a model of within-host pathogen evolution. In particular, we focused on the consequences of mismatched drug penetration, which may be common during combination therapy (22, 23, 25, 31). Our findings are summarized in Fig. 5.

In this model, mismatched penetration of two drugs into anatomical compartments sped up the evolution of multidrug resistance dramatically by creating zones of spatial monotherapy where only one drug from a combination regime is at therapeutic concentration. These zones, or "single-drug compartments," positively select for single-drug-resistant mutants, thereby favoring the fast stepwise accumulation of resistance mutations (Figs. 2 *A*, *B*, and *D* and 5*B*). Stepwise resistance evolution is hindered when drugs have identical penetration profiles, because in that case single-drug-resistant mutants compete with the fitter wild type in the sanctuary and they therefore suffer recurrent extinction (Figs. 2*C* and 5 *A* and *C*). Without access to the stepwise path, resistance mutations must be acquired near simultaneously; the system thus takes a far slower "direct" path to treatment failure. Even slight differences in penetration of coadministered drugs lead to a high risk of multidrug resistance, because the stepwise path dominates the direct path even for very small single-drug compartments (Fig. 2 *A* and *B*).

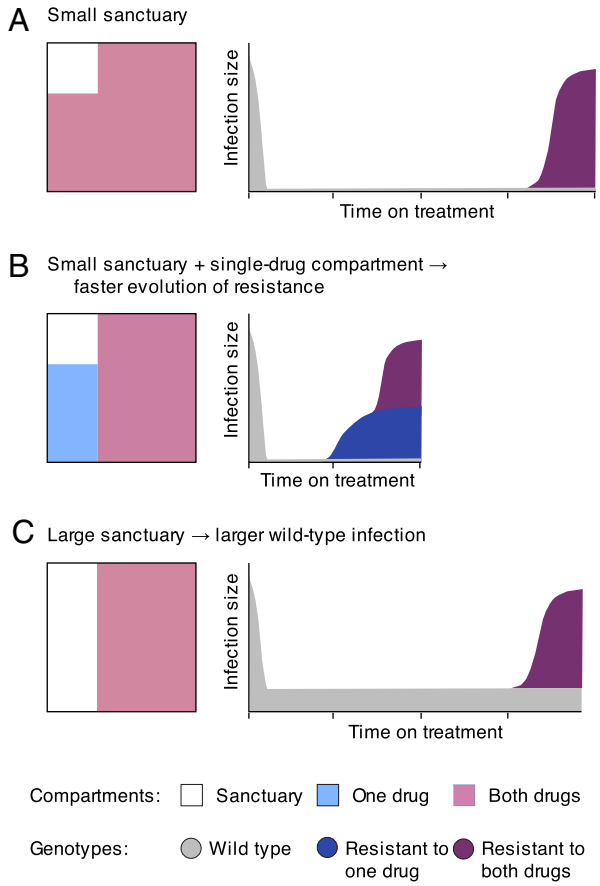

Fig. 5. Summary of the evolution of resistance with imperfect drug coverage. (*A*) When both drugs have high, matched penetration throughout the body, the evolution of multidrug resistance is slow, because it requires either preexisting multidrug resistance or near-simultaneous acquisition of both mutations along with migration out of a sanctuary site. If one drug (*B*) or both drugs (*C*) have a lower penetration, treatment outcomes may suffer in different ways. (*B*) If there are regions where only one drug reaches an effective concentration, then the evolution of multidrug resistance speeds up, because mutations may emerge in a stepwise fashion via single-drug compartments. Single mutations can arise de novo from a wild-type pathogen in the sanctuary or be selected from preexisting mutations in the single-drug compartment when treatment is started. (*C*) If the sanctuary is larger but both drugs reach the same regions of the body, then resistance still evolves slowly, but the infection size before treatment failure will be larger. Therefore, if high penetration of all drugs is impossible, there is a trade-off when choosing which drugs to pair in combinations: halting growth of the wild-type pathogen immediately (*B*) or preventing the sequential accumulation of resistance mutations (*C*).

The effects of single-drug compartments are most severe for chronic infections, during which pathogen replication persists to generate de novo resistance mutations, and treatment creates a long-term selective advantage for resistant strains. However, we have also demonstrated that mismatched penetration can speed up the development of resistance from preexisting mutations (Fig. 3) and can reduce the probability of cure for infections without a sanctuary (*SI Appendix*, Fig. S1), suggesting that these results may have applications to acute infections as well.

Although mismatched drug penetration generally favors resistance evolution and should be avoided, this may not always be possible. Immediate clinical efficacy may at times be more important than the prevention of resistance. It may therefore be advantageous, in some cases, to select a combination of drugs with different penetration profiles, if doing so eliminates sanctuary sites in the body. With no sanctuary sites, the total pathogen load will be as low as possible during treatment and few new mutations will be created. This slows the rate of evolution of drug resistance (Fig. 3) and makes complete eradication of the infection (cure) possible. If elimination of sanctuaries is not possible, however, then avoiding single-drug compartments due to mismatched penetration in a combination regime should be the main strategy for preventing multidrug resistance. If there are several single-drug compartments, eliminating one may have little effect if another remains. If neither single-drug compartments nor sanctuaries can be eliminated, then the optimal solution to reduce resistance is not obvious without some knowledge of the relevant parameters. Some insight as to where a particular treatment regime falls along this trade-off curve may be gained by observing the patterns of resistance acquisition. These include the overall prevalence of single-resistant strains before multidrug resistance emerges and the relative order in which different single-resistant strains appear. Previous work has questioned the orthodoxy that "aggressive" antimicrobial chemotherapy is optimal for preventing resistance (43, 50). If we consider that one aspect of treatment aggressiveness is the extent of drug penetration, then our model demonstrates the complexities involved in answering this question and motivates further work aimed at estimating the size of drug-protected compartments for relevant combination therapies.

In particular, our model offers an explanation for why the strategy suggested for some antibiotic treatments of pairing a broadly penetrating drug (e.g., rifampicin) with a narrowly penetrating one (e.g., vancomycin) to increase total drug coverage (51) might fail frequently due to the rapid evolution of resistance against the drug with higher penetration (51–53). It also offers an alternative explanation of why certain drugs are more vulnerable to resistance. This vulnerability is usually explained by a low genetic barrier to resistance (i.e., only one mutation needed) or by their long half-life. Our model suggests that broad penetration may also make a drug vulnerable to the evolution of resistance, if the drug is paired with drugs with lower penetration (Fig. 4).

Our model also offers an explanation of stepwise evolution of resistance in HIV infection, the commonly observed pattern whereby the virus gains one resistance mutation at a time (19, 54, 55). As treatment regimes are designed so that each drug is active against mutants resistant to the others, single-resistant mutants should be driven to extinction both in sanctuary zones (by competition with fitter wild type) and where all drugs are active (by sensitivity to all drugs save one). It has been hypothesized that either nonadherence to treatment or different drug half-lives cause "effective temporal monotherapy," which is to blame for the

appearance of single-drug-resistant viruses (16, 17). We propose that mismatched penetration of drugs in a combination treatment offers an alternative explanation for this stepwise evolution of resistance, via "effective spatial monotherapy." Very small single-drug compartments are sufficient to cause this effect, suggesting that these regions may be very hard to detect and could remain overlooked.

In this study, we focused on the case of treatment with two drugs, but we expect that our results could generalize to three or more different drugs. Adding a third drug to a regimen may reduce the size of the sanctuaries and/or the size of single-drug compartments and should therefore reduce the rate at which multidrug resistance evolves.

Several extensions to our model can be considered in future studies. First, we assume that drug compartments are discrete and have a fixed size; however, drug concentrations can be continuous in space and the pharmacokinetics of individual drugs can modify the size of the different compartments over time. Second, we have assumed that treatment fails when the double-drug compartment is invaded, but depending on the size and location of drug compartments in the body, treatment may fail when a single-drug compartment is invaded. Also, we assume a very specific migration model between the compartments [known in population genetics as the island model (56, 57)], but other migration models may be possible. Specifically, not all compartments may be connected by migration and the migration rates may be independent of the size of the target compartment.

Throughout this paper we have considered the fitness effect of multiple drugs or multiple mutations to be independent (Table 1), reducing the number of parameters in our model. Actual fitness landscapes may be more complex than this assumption allows. First, drugs may interact, so that their combined efficacy deviates from the product of their independent effects (58). Interactions may be synergistic, leading to greater reductions in pathogen fitness, or antagonistic, leading to smaller reductions (38, 39, 59–61). In the case where resistance mutations accumulate in compartments where both drugs are present, previous modeling and experimental studies have shown that extreme drug antagonism may hinder evolution of multidrug resistance (62, 63). In contrast to that case, we have shown here that when mutational costs are low (small s) and drugs are effective ($R_0 < 0.5$), treatment failure is far more likely to be caused by mutations generated in the absence of a drug that later migrate to a region where the drug penetrates. Therefore, for the scenarios considered in this study, we believe that these interactions have minimal effects as long as each drug is suppressive alone and in combination.

A second possible complication in the fitness landscape is that resistance mutations may interact, so that their combined fitness effects are not multiplicative, instead displaying patterns of epistasis. One type of interaction is cross-resistance, by which gaining resistance to one drug makes a pathogen strain either more or less susceptible to the other. Because positive cross-resistance (reduced susceptibility to the other drug) reduces the fitness gap between the single and double mutant in the presence of drugs, we would expect it to increase the rate of the stepwise path more than that of the direct path, hence amplifying the effect of single-drug compartments. Negative cross-resistance (increased susceptibility) conversely would diminish the stepwise path. A second type of interaction arises where costs of the resistance mutations are not independent, affecting their frequency (mutation–selection balance) in compartments lacking the drug. In many viral infections, the combined costs are lower than the product of individual costs (positive epistasis) (64–66). This scenario confers an advantage to double mutants, accelerating both paths to treatment failure, whereas negative epistasis would impede both paths.

Throughout this paper, we have assumed that no recombination (or any other form of lateral gene transfer) occurs between the two resistance loci. In general, recombination may increase or decrease the rate at which multiple-drug resistance develops (67, 68). However, two features of the clinical setting envisioned here minimize its importance to treatment failure. First, without epistasis, recombination will not meaningfully affect the individual gene frequencies (67). Second, in our model, there is no single compartment where the two resistance mutations are each beneficial individually, meaning that there is never a situation where both single mutants are common. As the two single mutants rarely contact one another, recombination cannot speed up the appearance of the double mutant beyond the action of mutation alone (68, 69).

Drug compartments are commonly described as specific anatomical locations in the body like organs or tissues. For instance, not all antimicrobial drugs penetrate to therapeutic concentrations in the central nervous system (22, 27, 28, 70), the genital tract (22, 25), the lymphoid tissue (22, 26), or other infected tissues (23, 48, 49). However, the compartments in our model could be interpreted in many ways. For example, they could represent different cell types, such as cells in a tumor that are not reached by anticancer drugs (71, 72), or phenotypically resistant subpopulations of bacteria that have low permeability to antibiotics (73) or replicate slowly (18, 37). The latter scenario was explored in a computational model of TB treatment (37) that analyzed the combined effect of noncompliance to treatment and heterogeneity in drug sensitivity due to differences in cell turnover rates. Overall this model is consistent with our results, finding that when patients were compliant to treatment, larger single-drug compartments led to more resistance. However, when patients followed a particular pattern of imperfect compliance to treatment—by stopping drugs once bacterial loads were below a threshold value—larger single-drug compartments actually slowed down resistance evolution. This occurred because the very slow antibiotic-mediated killing of cells in this compartment, due to the low cell turnover, meant that patients with larger compartments had to take drugs for much longer to reduce bacterial loads. Higher time-averaged drug loads understandably led to lower resistance risk. This comparison points out the importance of particular assumptions in determining outcomes and motivates further studies aimed at understanding the combined effect of spatial and temporal monotherapy.

Compartments could also exist at a population level, caused by interindividual differences in pharmacokinetic parameters (74) or differential targeting of geographic regions with insecticides, herbicides, or therapeutics. Finally, this model might be relevant to other evolutionary processes where multiple adaptations are ultimately needed for survival and to the study of the role of spatial heterogeneity in adaptation.

Materials and Methods

We use a basic viral dynamics model (40) to simulate the infection within each compartment and we include stochastic mutation and stochastic migration among all of the compartments. We perform exact stochastic simulations, tracking the genotype and location of every infected cell in the body and explicitly simulating all of the events that might occur to a cell: replication (representing either division of a bacterial cell or infection of a new cell by a virus), mutation (upon replication), death, and migration among different compartments. Simulations are performed using the Gillespie algorithm. Details of the model, analytic approximations, and simulation methods are provided in *SI Appendix*.

ACKNOWLEDGMENTS. The authors thank A. Harpak, P. Altrock, J. Wakeley, J. Hermisson, D. Weissman, H. Uecker, H. Alexander, B. Waclaw, S. van Doorn, and P. Abel zur Wiesch for helpful feedback on the project and the manuscript at various stages. S.M.-G. was funded by the Erasmus Mundus Masters Programme in Evolutionary Biology and by the European Research Council (Starting Grant 30955). A.L.H. and D.I.S.R. were supported by Bill and Melinda Gates Foundation Grand Challenges Explorations Grant OPP1044503. A.L.H. was also supported by National Institutes of Health (NIH) Grant DP5OD019851. D.A.P. was supported by NIH Grants RO1GM100366 and RO1GM097415. M.A.N. was supported by the John Templeton Foundation. P.S.P. received funding from the Human Frontiers Science Program (LT000591/2010-L).

1. Chernish RN, Aaron SD (2003) Approach to resistant gram-negative bacterial pulmonary infections in patients with cystic fibrosis. *Curr Opin Pulm Med* 9(6):509–515.
2. Gupta RK, et al. (2012) Global trends in antiretroviral resistance in treatment-naive individuals with HIV after rollout of antiretroviral treatment in resource-limited settings: A global collaborative study and meta-regression analysis. *Lancet* 380(9849): 1250–1258.
3. Tana MM, Ghany MG (2013) Hepatitis B virus treatment: Management of antiviral drug resistance. *Clin Liver Dis* 2(1):24–28.
4. Pawlotsky J-M (2011) Treatment failure and resistance with direct-acting antiviral drugs against hepatitis C virus. *Hepatology* 53(5):1742–1751.
5. Zumla A, et al. (2012) Drug-resistant tuberculosis—current dilemmas, unanswered questions, challenges, and priority needs. *J Infect Dis* 205(Suppl 2):S228–S240.
6. Holohan C, Van Schaeybroeck S, Longley DB, Johnston PG (2013) Cancer drug resistance: An evolving paradigm. *Nat Rev Cancer* 13(10):714–726.
7. Bozic I, et al. (2013) Evolutionary dynamics of cancer in response to targeted combination therapy. *eLife* 2(June):e00747.
8. Nijhuis M, et al. (1997) Lamivudine-resistant human immunodeficiency virus type 1 variants (184V) require multiple amino acid changes to become co-resistant to zidovudine in vivo. *J Infect Dis* 176(2):398–405.
9. Gulick RM, et al. (1998) Simultaneous vs sequential initiation of therapy with indinavir, zidovudine, and lamivudine for HIV-1 infection: 100-week follow-up. *JAMA* 280(1):35–41.
10. Yim HJ, et al. (2006) Evolution of multi-drug resistant hepatitis B virus during sequential therapy. *Hepatology* 44(3):703–712.
11. Zoulim F (2011) Hepatitis B virus resistance to antiviral drugs: Where are we going? *Liver Int* 31(Suppl 1):111–116.
12. Hedrick TL, et al. (2008) Outbreak of resistant *Pseudomonas aeruginosa* infections during a quarterly cycling antibiotic regimen. *Surg Infect* 9(2):139–152.
13. van Loon HJ, et al. (2005) Antibiotic rotation and development of gram-negative antibiotic resistance. *Am J Respir Crit Care Med* 171(5):480–487.
14. Abel zur Wiesch P, Kouyos R, Abel S, Viechtbauer W, Bonhoeffer S (2014) Cycling empirical antibiotic therapy in hospitals: Meta-analysis and models. *PLoS Pathog* 10(6):e1004225.
15. Hastings IM, Watkins WM, White NJ (2002) The evolution of drug-resistant malaria: The role of drug elimination half-life. *Philos Trans R Soc Lond B Biol Sci* 357(1420): 505–519.
16. Bangsberg DR, Kroetz DL, Deeks SG (2007) Adherence-resistance relationships to combination HIV antiretroviral therapy. *Curr HIV/AIDS Rep* 4(2):65–72.
17. Rosenbloom DI, Hill AL, Rabi SA, Siliciano RF, Nowak MA (2012) Antiretroviral dynamics determines HIV evolution and predicts therapy outcome. *Nat Med* 18(9): 1378–1385.
18. Mitchison DA (1998) How drug resistance emerges as a result of poor compliance during short course chemotherapy for tuberculosis. *Int J Tuberc Lung Dis* 2(1): 10–15.
19. Harrigan PR, et al. (2005) Predictors of HIV drug-resistance mutations in a large antiretroviral-naive cohort initiating triple antiretroviral therapy. *J Infect Dis* 191(3):339–347.
20. Bacheler LT, et al. (2000) Human immunodeficiency virus type 1 mutations selected in patients failing efavirenz combination therapy. *Antimicrob Agents Chemother* 44(9): 2475–2484.
21. Pennings PS (2012) Standing genetic variation and the evolution of drug resistance in HIV. *PLoS Comput Biol* 8(6):e1002527.
22. Solas C, et al. (2003) Discrepancies between protease inhibitor concentrations and viral load in reservoirs and sanctuary sites in human immunodeficiency virus-infected patients. *Antimicrob Agents Chemother* 47(1):238–243.
23. Dartois V (2014) The path of anti-tuberculosis drugs: From blood to lesions to mycobacterial cells. *Nat Rev Microbiol* 12(3):159–167.
24. Varatharajan L, Thomas SA (2009) The transport of anti-HIV drugs across blood-CNS interfaces: Summary of current knowledge and recommendations for further research. *Antiviral Res* 82(2):A99–A109.
25. Else LJ, Taylor S, Back DJ, Khoo SH (2011) Pharmacokinetics of antiretroviral drugs in anatomical sanctuary sites: The male and female genital tract. *Antivir Ther* 16(8): 1149–1167.
26. Fletcher CV, et al. (2014) Persistent HIV-1 replication is associated with lower antiretroviral drug concentrations in lymphatic tissues. *Proc Natl Acad Sci USA* 111(6): 2307–2312.
27. Antinori A, et al. (2005) Efficacy of cerebrospinal fluid (CSF)-penetrating antiretroviral drugs against HIV in the neurological compartment: Different patterns of phenotypic resistance in CSF and plasma. *Clin Infect Dis* 41(12):1787–1793.
28. Edén A, et al. (2010) HIV-1 viral escape in cerebrospinal fluid of subjects on suppressive antiretroviral treatment. *J Infect Dis* 202(12):1819–1825.
29. van Lelyveld SF, et al. (2010) Therapy failure following selection of enfuvirtide-resistant HIV-1 in cerebrospinal fluid. *Clin Infect Dis* 50(3):387–390.
30. Singh R, Ray P, Das A, Sharma M (2010) Penetration of antibiotics through *Staphylococcus aureus* and *Staphylococcus epidermidis* biofilms. *J Antimicrob Chemother* 65(9):1955–1958.
31. Deresinski S (2009) Vancomycin in combination with other antibiotics for the treatment of serious methicillin-resistant *Staphylococcus aureus* infections. *Clin Infect Dis* 49(7):1072–1079.
32. Kepler TB, Perelson AS (1998) Drug concentration heterogeneity facilitates the evolution of drug resistance. *Proc Natl Acad Sci USA* 95(20):11514–11519.
33. Greulich P, Waclaw B, Allen RJ (2012) Mutational pathway determines whether drug gradients accelerate evolution of drug-resistant cells. *Phys Rev Lett* 109(8):088101.
34. Hermsen R, Deris JB, Hwa T (2012) On the rapidity of antibiotic resistance evolution facilitated by a concentration gradient. *Proc Natl Acad Sci USA* 109(27): 10775–10780.
35. Zhang Q, et al. (2011) Acceleration of emergence of bacterial antibiotic resistance in connected microenvironments. *Science* 333(6050):1764–1767.
36. Toprak E, et al. (2012) Evolutionary paths to antibiotic resistance under dynamically sustained drug selection. *Nat Genet* 44(1):101–105.
37. Lipsitch M, Levin BR (1998) Population dynamics of tuberculosis treatment: Mathematical models of the roles of non-compliance and bacterial heterogeneity in the evolution of drug resistance. *Int J Tuberc Lung Dis* 2(3):187–199.
38. Ankomah P, Levin BR (2012) Two-drug antimicrobial chemotherapy: A mathematical model and experiments with *Mycobacterium marinum*. *PLoS Pathog* 8(1): e1002487.
39. Ankomah P, Johnson PJT, Levin BR (2013) The pharmaco-, population and evolutionary dynamics of multi-drug therapy: Experiments with *S. aureus* and *E. coli* and computer simulations. *PLoS Pathog* 9(4):e1003300.
40. Nowak MA, May RMC (2000) *Virus Dynamics: Mathematical Principles of Immunology and Virology* (Oxford Univ Press, New York).
41. Iwasa Y, Michor F, Nowak MA (2004) Stochastic tunnels in evolutionary dynamics. *Genetics* 166(3):1571–1579.
42. Weissman DB, Desai MM, Fisher DS, Feldman MW (2009) The rate at which asexual populations cross fitness valleys. *Theor Popul Biol* 75(4):286–300.
43. Kouyos RD, et al. (2014) The path of least resistance: Aggressive or moderate treatment? *Proc R Soc B Biol Sci* 281(1794):20140566.
44. Bonhoeffer S, Nowak MA (1997) Pre-existence and emergence of drug resistance in HIV-1 infection. *Proc Biol Sci* 264(1382):631–637.
45. Ribeiro RM, Bonhoeffer S, Nowak MA (1998) The frequency of resistant mutant virus before antiviral therapy. *AIDS* 12(5):461–465.
46. Alexander HK, Bonhoeffer S (2012) Pre-existence and emergence of drug resistance in a generalized model of intra-host viral dynamics. *Epidemics* 4(4):187–202.
47. Orr HA, Unckless RL (2008) Population extinction and the genetics of adaptation. *Am Nat* 172(2):160–169.
48. Müller M, dela Peña A, Derendorf H (2004) Issues in pharmacokinetics and pharmacodynamics of anti-infective agents: Distribution in tissue. *Antimicrob Agents Chemother* 48(5):1441–1453.
49. Joukhadar C, et al. (2001) Impaired target site penetration of beta-lactams may account for therapeutic failure in patients with septic shock. *Crit Care Med* 29(2): 385–391.
50. Read AF, Day T, Huijben S (2011) The evolution of drug resistance and the curious orthodoxy of aggressive chemotherapy. *Proc Natl Acad Sci USA* 108(Suppl 2):10871–10877.
51. Jung YJ, et al. (2010) Effect of vancomycin plus rifampicin in the treatment of nosocomial methicillin-resistant *Staphylococcus aureus* pneumonia. *Crit Care Med* 38(1): 175–180.
52. Simon GL, Smith RH, Sande MA (1983) Emergence of rifampin-resistant strains of *Staphylococcus aureus* during combination therapy with vancomycin and rifampin: A report of two cases. *Rev Infect Dis* 5(Suppl 3):S507–S508.
53. Mwangi MM, et al. (2007) Tracking the *in vivo* evolution of multidrug resistance in *Staphylococcus aureus* by whole-genome sequencing. *Proc Natl Acad Sci USA* 104(22): 9451–9456.
54. Pennings PS, Kryazhimskiy S, Wakeley J (2014) Loss and recovery of genetic diversity in adapting populations of HIV. *PLoS Genet* 10(1):e1004000.
55. UK Collaborative Group on HIV Drug Resistance; UK CHIC Study Group (2010) Long-term probability of detecting drug-resistant HIV in treatment-naive patients initiating combination antiretroviral therapy. *Clin Infect Dis* 50(9):1275–1285.
56. Wright S (1943) Isolation by distance. *Genetics* 28(2):114–138.
57. Uecker H, Otto SP, Hermisson J (2014) Evolutionary rescue in structured populations. *Am Nat* 183(1):E17–E35.
58. Bliss CI (1939) The toxicity of poisons applied jointly. *Ann Appl Biol* 26(3):585–615.
59. Greco WR, Bravo G, Parsons JC (1995) The search for synergy: A critical review from a response surface perspective. *Pharmacol Rev* 47(2):331–385.
60. Jilek BL, et al. (2012) A quantitative basis for antiretroviral therapy for HIV-1 infection. *Nat Med* 18(3):446–451.
61. Ocampo PS, et al. (2014) Antagonism between bacteriostatic and bactericidal antibiotics is prevalent. *Antimicrob Agents Chemother* 58(8):4573–4582.
62. Michel J-B, Yeh PJ, Chait R, Moellering RC, Jr, Kishony R (2008) Drug interactions modulate the potential for evolution of resistance. *Proc Natl Acad Sci USA* 105(39): 14918–14923.
63. Chait R, Craney A, Kishony R (2007) Antibiotic interactions that select against resistance. *Nature* 446(7136):668–671.
64. Sanjuán R, Moya A, Elena SF (2004) The contribution of epistasis to the architecture of fitness in an RNA virus. *Proc Natl Acad Sci USA* 101(43):15376–15379.
65. Bonhoeffer S, Chappey C, Parkin NT, Whitcomb JM, Petropoulos CJ (2004) Evidence for positive epistasis in HIV-1. *Science* 306(5701):1547–1550.
66. Holmes EC (2009) *Evolution and Emergence of RNA Viruses* (Oxford Univ Press, New York).
67. Bretscher MT, Althaus CL, Müller V, Bonhoeffer S (2004) Recombination in HIV and the evolution of drug resistance: For better or for worse? *BioEssays* 26(2):180–188.
68. Carvajal-Rodríguez A, Crandall KA, Posada D (2007) Recombination favors the evolution of drug resistance in HIV-1 during antiretroviral therapy. *Infect Genet Evol* 7(4): 476–483.
69. Althaus CL, Bonhoeffer S (2005) Stochastic interplay between mutation and recombination during the acquisition of drug resistance mutations in human immunodeficiency virus type 1. *J Virol* 79(21):13572–13578.

70. Kearney BP, Aweeka FT (1999) The penetration of anti-infectives into the central nervous system. *Neurol Clin* 17(4):883–900.
71. Minchinton AI, Tannock IF (2006) Drug penetration in solid tumours. *Nat Rev Cancer* 6(8):583–592.
72. Fu F, Nowak MA, Bonhoeffer S (2015) Spatial heterogeneity in drug concentrations can facilitate the emergence of resistance to cancer therapy. *PLoS Comput Biol* 11(3):e1004142.
73. Sarathy J, Dartois V, Dick T, Gengenbacher M (2013) Reduced drug uptake in phenotypically resistant nutrient-starved nonreplicating *Mycobacterium tuberculosis*. *Antimicrob Agents Chemother* 57(4):1648–1653.
74. Srivastava S, Pasipanodya JG, Meek C, Leff R, Gumbo T (2011) Multidrug-resistant tuberculosis not due to noncompliance but to between-patient pharmacokinetic variability. *J Infect Dis* 204(12):1951–1959.

SUPPLEMENTARY INFORMATION

Imperfect drug penetration leads to spatial monotherapy and rapid evolution of multi-drug resistance

Stefany Moreno-Gamez[1,2,*], Alison L. Hill[1,*], Daniel I. S. Rosenbloom[1,3], Dmitri A. Petrov[4], Martin A. Nowak[1], and Pleuni Pennings[5]

[1]Program for Evolutionary Dynamics, Department of Mathematics, Department of Organismic and Evolutionary Biology, Harvard University, Cambridge, MA 02138, USA
[2]Theoretical Biology Group, Groningen Institute for Evolutionary Life Sciences, University of Groningen, Groningen, 9747 AG, The Netherlands
[3]Department of Biomedical Informatics, Columbia University Medical Center, New York, NY 10032, USA
[4]Department of Biology, Stanford University, Stanford, CA 94305, USA
[5]Department of Biology, San Francisco State University, San Francisco, CA 94132, USA
[*]These authors contributed equally to the manuscript

May 7, 2015

Contents

Part I
Basic results of the viral dynamics model

1 Deterministic model

In the absence of mutation or migration, the dynamics for a virus of strain i, present in compartment j, can be described using the basic viral dynamics equations (1):

$$\begin{aligned} \dot{x_j} &= \lambda_j - \beta_{ij} x_j v_{ij} - d_x x_j \\ \dot{y_{ij}} &= \beta_{ij} x_j v_{ij} - d_y y_{ij} \\ \dot{v_{ij}} &= k y_{ij} - d_v v_{ij} \end{aligned} \tag{1}$$

where x_j, y_{ij} and v_{ij} are the populations of uninfected cells, cells infected with strain i and free virus of strain i, respectively - all in compartment j. Uninfected host cells die at rate d_x and are produced at rate λ_j. These cells become infected by strain i at rate β_{ij}. Infected cells die at rate d_y and produce free virus at rate k. Free virus is cleared at rate d_v. Implicit in these parameter choices is the assumption that compartments differ only in the rate at which uninfected cells are produced, and viral strains differ only in the rate at which they infect new cells.

The *basic reproductive ratio* (i.e. the number of new infections generated by an infected cell before it dies in a totally susceptible population of host cells) for this model is $R_0^{ij} = \lambda_j \beta_{ij} k/(d_x d_y d_v)$ (Ref (1)).

This system can be simplified by assuming that the population of free virus instantaneously reaches an equilibrium with respect to the population of infected cells. This separation of timescales is valid when we are not interested in short term fluctuations, because the dynamics of the virus tend to be much faster than those of cells (1; 2). We therefore set $\dot{v_{ij}} = 0$ and get $v = (k/d_v)y$, and by defining $B_{ij} = \beta_{ij} k/d_v$ we reduce the model to two equations tracking only cells:

$$\begin{aligned} \dot{x_j} &= \lambda_j - B_{ij} x_j y_{kj} - d_x x_j \\ \dot{y_{ij}} &= B_{ij} x_j y_{ij} - d_y y_{ij} \end{aligned} \tag{2}$$

There are two steady state solutions to this system of equations when only a single strain is present: When $R_0^{ij} \equiv \lambda_j B_{ij}/(d_x d_y) < 1$, there is no infection, and when $R_0^{ij} > 1$, the infection reaches a steady state level:

$$\{x_j^*, y_{ij}^*\} = \begin{cases} \left\{ \dfrac{\lambda_j}{d_x}, 0 \right\} \equiv \{N_j, 0\} & \text{if } R_0^{ij} < 1 \\ \left\{ \dfrac{N_j}{R_0^{ij}}, \dfrac{N_j d_x}{d_y} \left(1 - \dfrac{1}{R_0^{ij}} \right) \right\} \equiv \left\{ \dfrac{N_j}{R_0^{ij}}, K_j^i \right\} & \text{if } R_0^{ij} > 1 \end{cases} \tag{3}$$

When there is more than one virus strain in a single compartment at a given time, the equations can easily be modified and new steady state solutions and stability conditions derived. The result is that only one virus strain ever remains in the compartment at steady state (competitive exclusion) (1). This is the strain with the highest R_0 value.

These steady state equations give rise to terms we will frequently use throughout the paper. The total number of uninfected host cells that a compartment j contains when there is no virus present is called the *compartment size* and is given by N_j. The equilibrium number of infected cells of type i that are present in a compartment when $R_0^{ij} > 1$ for strain i and $R_0^{ij} > R_0^{kj}$ for all $k \neq i$ is termed the *carrying capacity* and is denoted by K_j^i.

This system can be extended to account for mutation and migration, along with the presence of multiple strains:

$$\begin{aligned} \dot{x_j} &= \lambda_j - x_j \sum_k B_{kj} y_{kj} - d_x x_j \\ \dot{y_{ij}} &= x_j \sum_k \mu_{ki} B_{kj} y_{kj} - (d_y + \sum_q m_{jq}) y_{ij} + \sum_q m_{qj} y_{iq} \end{aligned} \tag{4}$$

where μ_{ki} is the probability per infection event that strain k mutates to strain i, and m_{qj} is the rate of migration from compartment q to compartment j. Note that we have ignored the migration of uninfected cells, since it is not important for the evolutionary process we are interested in. Because we are only tracking cells, and not virus, we have implicitly assumed that it is infected cells that migrate. This assumption should have only miminal influence on our results, because while virus numbers are much larger than those of infected cells, the establishment probability starting from a single virion is much lower.

This system no longer yields a tractable analytic solution when $R_0^{ij} > 1$ for any $\{i, j\}$, and in general is better described by a stochastic process, since we will mainly be interested in the time until equilibrium is reached. The result of mutation and migration is that the equilibrium levels will be altered compared to Eq. (3). The major qualitative difference is that strains will persist in compartments where $R_0^{ij} < 1$. When u and m are small, these levels tend to be very low compared to the N_j and K_j^i, and differences in $\{x_j^*, y_{ij}^*\}$ from Eq. (3) are minor. However, as this paper demonstrates, mutation, migration and the relative viral fitness values in different compartments have a major influence on the *time* to reach the equilibrium state.

While in general the migration rates m_{qj} can take on any values, we choose a simple and biologically realistic migration scheme to reduce the number of independent parameters. In this scheme, each pathogen migrates out of its current compartment at rate m. Migrants from a given compartment are then distributed into all four compartments (including the one they came from) proportionally to the compartment sizes, so that larger compartments get more migrants. Therefore, the rate of migration from compartment q to compartment j becomes

$$m_{qj} = m \frac{N_j}{N_{TOT}} \tag{5}$$

where $N_{TOT} = \sum_j N_j$ is the total number of uninfected host cells in the body before infection.

2 Stochastic model

The deterministic viral dynamics model tracking uninfected and infected cells serves well to describe the growth of the infection when the number of cells of any type is large, however, when cell numbers are small, such as when the infection initially starts or when a new strain arises, stochastic effects become important. The deterministic model can be reformulated as a branching process (similar to (3–5)) during these initial stages of infection, since the number of uninfected target cells (x) is approximately constant on this timescale:

$$\begin{aligned} Y_{ij} &\to Y_{ij} + 1 \text{ ... rate: } R_0^{ij} d_y \\ Y_{ij} &\to Y_{ij} - 1 \text{ ... rate: } d_y. \end{aligned} \tag{6}$$

This is a standard birth-death process. Note that there are an infinite number of stochastic processes that reduce to the same deterministic equations, and for some infections, burst-death models (5–7) - where many new infections occur from a single infection nearly simulataneously - may be more appropriate. To keep our model general and to ensure closed form solutions for the probabalistic expressions described below, we have chosen the simplest process.

If a single cell infected with strain i arrives in compartment j where it has $R_0^{ij} > 1$, then the probability it will grow to establish an infection (described by Equation 3) as opposed to going extinct(8) is

$$P_{est}^{ij} = 1 - \frac{1}{R_0^{ij}}. \tag{7}$$

If a single cell infected with strain i arrives in compartment j where it has $R_0^{ij} < 1$, then $P_{est}^{ij} = 0$ but this cell may still infect a few other cells before the infection dies off. The average number of new infections caused by a single infected cell is

$$E[X_{ij}] = \frac{R_0^{ij}}{1 - R_0^{ij}}. \tag{8}$$

Note that Eq. (8) does not count the initial migrant cell, only new infections that occur in compartment j.

This equation makes use of the fact that the probability of producing exactly n offspring is given by

$$\begin{aligned} P(n_{ij}) &= C_n \frac{(R_0^{ij})^n}{(1 + R_0^{ij})^{2n+1}} \\ C_n &= \frac{1}{1+n} \binom{2n}{n}. \end{aligned}$$

where C_n is the n_{th} Catalan number, describing the number of unique infection paths leading to exactly n offspring.

It is important to note that both these equations apply only when there is no previously established infection when the initial cell of strain i arrives. If strain $k \neq i$ is already resident in compartment j, then R_0^{ij} must be replaced by R_0^{ij}/R_0^{kj}, to account for the reduction in target cells (see x^* in Equation 3).

3 Mutation-selection equilibrium

To approximate the probability of resistance via different paths in later sections, we will encounter many expressions that require the frequency at which a rare deleterious mutant exists in a population at equilibrium. Here we describe a method to determine the probability distribution for the number of either one-step or two-step mutants in a compartment where the wild-type (or single mutant) population is at carrying capacity.

We make the following assumptions: The carrying capacity of the resident population is large enough that stochastic fluctuations in size are not important. At each infection event, there is a probability μ that a wild-type infected cell will mutate and instead produce a mutant infected cell. Mutant cells have a infection rate that is reduced by a factor of $1-s$, where $0 < s < 1$ is the cost of the mutation (or the selection coefficient), but die at the same rate d_y. We can assume that $\mu << 1$ so that mutation does not significantly change the equilibrium population size nor the infection rate of the wild-type cells.

3.1 Frequency of single mutants

Here we consider, as an example, mutants resistant to drug 1 that exist before treatment, or in the sanctuary during treatment. The frequency of single mutants can be determined by considering the stochastic process determining the size of the single mutant population (X_1). Let the resident population (in this example, the wild type) be at equilibrium level (K), where the replication rate is equal to the death rate ($d_y K$). We then have the following processes that can stochastically occur in the population:

$$\begin{aligned} X_1 &\rightarrow X_1 + 1 \text{ ... rate: } \mu_1 d_y K \\ X_1 &\rightarrow X_1 + 1 \text{ ... rate: } (1-s_1) d_y X_1 \\ X_1 &\rightarrow X_1 - 1 \text{ ... rate: } d_y X_1 \end{aligned} \tag{9}$$

This is a standard immigration-birth-death process, with immigration rate $I = \mu_1 d_y K$, birth rate $B = (1-s_1)d_y$, and death rate $D = d_y$. The probability generating function for the the size of a population governed by this process (9; 10) is

$$F(z) = \left(\frac{B-D}{Bz-D} \right)^{\left(\frac{I}{B}\right)} \tag{10}$$

and so the PGF for the distribution of the mutant population size is

$$F(z) = \left(\frac{s_1}{1-(1-s_1)z} \right)^{\left(\frac{K\mu_1}{(1-s_1)}\right)} \tag{11}$$

where the probability that there are exactly n mutants can be recovered as $p(n) = \frac{1}{n!}\frac{d^n F}{dz^n}|_{z=0}$. The average number of mutants is

$$E[z] = \frac{dF}{dz}|_{z=1} = K\frac{\mu_1}{s_1}. \tag{12}$$

3.2 Frequency of double mutants

We now assume that one mutation occurs at a rate μ_1 and has cost s_1, while the other has μ_2 and s_2. This situation represents the occurance of double mutants in any compartment before treatment starts or in the sanctuary during treatment. A cell with both mutations can arise by either by a wild-type cell acquiring both mutations simultaneously, or, by a mutant cell with one mutation gaining the other (in either order). The fitness of the double mutant cells is reduced by a factor $(1-s_1)(1-s_2)$.

The frequency of double mutants can be determined by considering the stochastic process determining the size of the single and double mutant populations (X_1, X_2, X_{12}):

$$\begin{aligned}
X_1 &\to X_1 + 1 \text{ ... rate: } \mu_1 d_y K + (1-s_1) d_y X_1 \\
X_1 &\to X_1 - 1 \text{ ... rate: } d_y X_1 \\
X_2 &\to X_2 + 1 \text{ ... rate: } \mu_2 d_y K + (1-s_2) d_y X_2 \\
X_2 &\to X_2 - 1 \text{ ... rate: } d_y X_2 \\
X_{12} &\to X_{12} + 1 \text{ ... rate: } \mu_1\mu_2 d_y K + \mu_1(1-s_2) d_y X_2 + \mu_2(1-s_1) d_y X_1 + (1-s_1)(1-s_2) d_y X_{12} \\
X_{12} &\to X_{12} - 1 \text{ ... rate: } d_y X_{12}
\end{aligned} \tag{13}$$

However, this is no longer a simple immigration-birth-death process and we are not aware of an analytic solution.

An approximate solution can be obtained if we assume that each of the single mutant populations are large enough so that they can also be considered to be at a constant equilibrium level ($K_1 = \mu_1/s_1 K$ and $K_2 = \mu_2/s_2 K$). This approximation is reasonable, because if double mutants are frequent enough to affect treatment failure, then for realistically small values of μ/s , single mutants will be quite frequent.

In this limit, the stochastic process is now:

$$\begin{aligned} &X_{12} \to X_{12} + 1 \text{ ... rate: } \mu_1\mu_2 d_y K + \mu_1(1-s_2)d_y\left(\frac{\mu_2}{s_2}\right)K + \mu_2(1-s_1)d_y\left(\frac{\mu_1}{s_1}\right)K \\ &X_{12} \to X_{12} + 1 \text{ ... rate: } (1-s_1)(1-s_2)d_y X_{12} \\ &X_{12} \to X_{12} - 1 \text{ ... rate: } d_y X_{12} \end{aligned} \tag{14}$$

This is a modified immigration-birth-death process with

$$\begin{aligned} I &= \mu_1\mu_2 d_y K\left(\frac{1}{s_1} + \frac{1}{s_2} - 1\right) \\ B &= (1-s_1)(1-s_2)d_y \\ D &= d_y \end{aligned} \tag{15}$$

and the PGF for the distribution of the double mutant population size is

$$F(z) = \left(\frac{1-(1-s_1)(1-s_2)}{1-(1-s_1)(1-s_2)z}\right)^{\frac{\mu_1\mu_2}{(1-s_1)(1-s_2)}K\left(\frac{1}{s_1}+\frac{1}{s_2}-1\right)} \tag{16}$$

where the probability that there are exactly n mutants can be recovered as $p(n) = \frac{1}{n!}\frac{d^n F}{dz^n}|_{z=0}$. The average number of mutants is

$$E[z] = K\frac{\mu_1\mu_2}{s_1 s_2}. \tag{17}$$

This is the same result that one would derive using a fully deterministic model (for example, see Nowak and May(1)).

Part II
Paths to treatment failure

4 Overview of probability of treatment failure

To obtain a simplified analytic description of the probability distribution of the time to treatment failure in our model, we consider a reduced Markov chain description for the evolution of resistance. The Markov chain reduces the possible number of states of the population using the following assumptions: First, we assume that only one type of cells is present in a compartment at a given time. Second, we assume that when a strain that colonizes a compartment, it instantaneously reaches its carrying capacity. This means that the period when the strain is growing exponentially is ignored. We can make this assumption because exponential growth occurs much faster than evolution (separation of timescales), so the chance that resistance mutations appear when the pathogen is growing exponentially is much lower than the chance that they appear when the infected cells are at carrying capacity. Thus, in this description a compartment is either empty or fully occupied

by only one strain. Transitions between states in this description occur at constant rates given by their average value.

In the simplest case, we will consider two competing paths to resistance: *direct evolution* of double-drug resistance from the sanctuary, or *stepwise evolution* of resistance via the single-drug compartment. For simplicity, **for the rest of the Supplement we will assume there is only one single-drug compartment**, with drug 1, though extension to two is straightforward. We will first derive results without considering the possibility of pre-existing mutations, and then extend our calculations to include this source.

4.1 Acquired resistance only

Let r_{01} be the probability per unit time (the rate) at which the single-drug compartment ("1") is colonized from the sanctuary ("0"). Similarly, r_{12} is the rate of the double-drug compartment ("2") being colonized from the single-drug compartment (once the SDC is colonized), and r_{02} the rate of direct colonization of the double-drug compartment from the sanctuary. Expressions for these rates will be given in the subsequent sections (§5.1-5.3). Assuming that at $t = 0$ only the sanctuary is colonized, and it contains only wild-type cells at carrying capacity, then we can write the probability distribution functions for the time at which the double-drug compartment is colonized via each path as

$$\begin{aligned} P_{02}(t) &= r_{02}e^{-r_{02}t} \\ P_{012}(t) &= \frac{r_{01}r_{12}}{r_{01}-r_{12}}(e^{-r_{12}t} - e^{-r_{01}t}) \end{aligned} \tag{18}$$

where P_{02} refers to the direct path from the sanctuary, and P_{012} refers to the path going through the single-drug compartment. Similarly, the cumulative distribution functions $C(t)$, defined as the probability that the target compartment has already been colonized by a particular time, are written as $C(t) = \int_0^t P(u)du$.

The conditional cumulative distribution function $F(t)$ describes the probability that the double-drug compartment is colonized via a particular path, by a particular time, when both paths are possible. To calculate $F(t)$, we must condition the CDF for each path on the probability that the other path has *not* occurred, resulting in

$$\begin{aligned} F_{02}(t) &= \int_0^t P_{02}(u)(1 - C_{012}(u))du \\ F_{012}(t) &= \int_0^t P_{012}(u)(1 - C_{02}(u))du \end{aligned} \tag{19}$$

4.2 Including pre-existing resistance

At the time that drug treatment is started, there may already be single mutants pre-existing in the single-drug compartment, or double mutants pre-existing in the double-drug compartment, which

can speed up the time to resistance. We term the probability that an individual has an established single mutant population in the single-drug compartment at $t = 0$ as p_{ss} and the same probability for a double mutant in the double-drug compartment as p_{dd}. Then the conditional cumulative distribution functions become

$$\begin{aligned} F_{02}(t) &= (1 - p_{ss}) \left(p_{dd} + (1 - p_{dd}) \int_0^t P_{02}(u)(1 - C_{012}(u))du \right) \\ F_{012}(t) &= p_{ss} + (1 - p_{ss})(1 - p_{dd}) \int_0^t P_{012}(u)(1 - C_{02}(u))du \end{aligned} \tag{20}$$

5 Rates of treatment failure

5.1 Colonization of the single-drug compartment by single resistant mutants

For each single-drug compartment, there are two separate paths by which single drug resistance can arise during treatment, depending on whether mutation or migration from the sanctuary occurs first. Consequently, in the general two-drug case where there are two single-drug compartments, there are four separate paths by which single-drug resistance can happen. Here we present results only considering one single-drug compartment, though the extension to two is simple. Parameter descriptions are given in the main text.

Mutation-migration path In this path a mutant strain is generated in the sanctuary and migrates to the single-drug compartment. The rate at which this path happens is proportional to the carrying capacity of the wild-type population in the sanctuary (number of infected cells at equilibrium), the frequency of the mutant in this population (Equation 12), the migration rate (Equation 5), and the establishment probability (Equation 7) of the mutant in the single-drug compartment:

$$\begin{aligned} r_{01}^{\mu m} &= K_{SAN}^{WT} \frac{\mu_1}{s_1} m_{SAN,SDC} P_{est}^{1,SDC} \\ &= K_{SAN}^{WT} \frac{\mu_1}{s_1} m \frac{N_{SDC}}{N_{TOT}} \left(1 - \frac{1}{R_{WT}(1 - s_1)} \right) \end{aligned} \tag{21}$$

Migration-mutation path In this path a wild-type migrant from the sanctuary goes to the single-drug compartment and gains a mutation. The rate at which this path happens is proportional to the carrying capacity of the wild-type population in the sanctuary (number of infected cells at equilibrium), the migration rate, the size of the wild-type infection in the single-drug compartment before it goes extinct (Equation 8), the mutation rate, and the establishment probability of the mutant.

$$\begin{aligned} r_{01}^{m\mu} &= K_{SAN}^{WT} m_{SAN,SDC} E[X_{WT,SDC}] \mu_1 P_{est}^{1,SDC} \\ &= K_{SAN}^{WT} m \frac{N_{SDC}}{N_{TOT}} \left(\frac{R_{WT}(1 - \epsilon_1)}{1 - R_{WT}(1 - \epsilon_1)} \right) \mu_1 \left(1 - \frac{1}{R_{WT}(1 - s_1)} \right) \end{aligned} \tag{22}$$

Comparison The total rate of colonization is $r_{01} = r_{01}^{\mu m} + r_{01}^{m\mu}$. For most of the parameter ranges we will consider, the rate of the mutation-migration path is much larger than the rate of the migration-mutation path. This is because we consider the cost of the mutation (s) to be relatively small but the drug efficacy to be quite large ($\epsilon \approx 1$), so that the fitness of the mutant in the sanctuary is much larger than the fitness of the wild type in the single-drug compartment. However, if $R_{WT}(1-\epsilon_1) > 0.5$, it is possible for the migration-mutation path to be more important.

5.2 Colonization of the double-drug compartment via the single-drug compartment

There are two separate paths by which double drug resistance can arise from single mutants established the SDC during treatment, depending on whether mutation or migration from the SDC occurs first.

Mutation-migration path In this path a double mutant strain is generated in the single-drug compartment and migrates to the double-drug compartment. We assume the single resistant population in the single-drug compartment is at steady state when mutation occurs. The rate at which this path happens is proportional to the carrying capacity of the single resistant mutant population in the single-drug compartment (number of infected cells at equilibrium), the frequency of the double mutant in this population, the migration rate, and the establishment probability of the double mutant in the double-drug compartment.

$$\begin{aligned} r_{12}^{\mu m} &= K_{SDC}^{1} \frac{\mu_2}{s_2} m_{SDC,DDC} P_{est}^{12,DDC} \\ &= K_{SDC}^{1} \frac{\mu_2}{s_2} m \frac{N_{DDC}}{N_{TOT}} \left(1 - \frac{1}{R_{WT}(1-s_1)(1-s_2)}\right) \end{aligned} \tag{23}$$

Migration-mutation path In this path a single resistant mutant migrant from the single-drug compartment goes to the double-drug compartment and gains a mutation. We assume the single resistant population in the single-drug compartment is at steady state when migration occurs. The rate at which this path happens is proportional to the carrying capacity of the single resistant mutant population in the single-drug compartment (number of infected cells at equilibrium), the migration rate, the size of the single resistant infection in the double-drug compartment before it goes extinct, the mutation rate, and the establishment probability of the double mutant.

$$\begin{aligned} r_{12}^{m\mu} &= K_{SDC}^{1} m_{SDC,DDC} E[X_{1,DDC}] \mu_2 P_{est}^{12,DDC} \\ &= K_{SDC}^{1} m \frac{N_{DDC}}{N_{TOT}} \left(\frac{R_{WT}(1-s_1)(1-\epsilon_2)}{1 - R_{WT}(1-s_1)(1-\epsilon_2)}\right) \mu_2 \left(1 - \frac{1}{R_{WT}(1-s_1)(1-s_2)}\right) \end{aligned} \tag{24}$$

Comparison The total rate of colonization is $r_{12} = r_{12}^{\mu m} + r_{12}^{m\mu}$. For most of the parameter ranges we will consider, the rate of the mutation-migration path is much larger than the rate of the migration-mutation path. This is because we consider the cost of the mutation (s_2) to be

relatively small but the drug efficacy to be quite large ($\epsilon_2 \approx 1$), so that the fitness of the mutant in the SANctuary is much larger than the fitness of the wild type in the single-drug compartment. However, if $R_{WT}(1-\epsilon_2) > 0.5$, it is possible for the migration-mutation path to be more important.

5.3 Colonization of the double-drug compartment directly from the sanctuary

There are three separate paths by which double drug resistance can arise directly from the sanctuary during treatment, depending on the order in which the two mutations are acquired relative to the migration event from the sanctuary.

Mutation-mutation-migration path In this path a double mutant strain is generated in the sanctuary and migrates to the double-drug compartment. The rate at which this path happens is proportional to the carrying capacity of the wild-type population in the sanctuary (the number of infected cells at equilibrium), the frequency of the double mutant in this population, the migration rate, and the establishment probability of the double mutant in the double-drug compartment.

$$\begin{aligned} r_{02}^{\mu\mu m} &= K_{SAN}^{WT} \frac{\mu_1 \mu_2}{s_1 s_2} m_{SAN,DDC} P_{est}^{12,DDC} \\ &= K_{SAN}^{WT} \frac{\mu_1 \mu_2}{s_1 s_2} m \frac{N_{DDC}}{N_{TOT}} \left(1 - \frac{1}{R_{WT}(1-s_1)(1-s_2)}\right) \end{aligned} \tag{25}$$

Mutation-migration-mutation path In this path a single mutant strain resistant to either drug 1 or drug 2 is generated in the sanctuary and migrates to the double-drug compartment, where it gains a second mutation. The rate at which this path happens is proportional to the carrying capacity of the wild-type population in the sanctuary (the number of infected cells at equilibrium), the frequency of the single mutant in this population, the migration rate, the size of the single mutant infection in the double-drug compartment before going extinct, the mutation rate, and the establishment probability of the double mutant in the double-drug compartment. Mutations can occur in either order.

$$\begin{aligned} r_{02}^{\mu m \mu} &= K_{SAN}^{WT} \frac{\mu_1}{s_1} m_{SAN,DDC} E[X_{1,DDC}] \mu_2 P_{est}^{12,DDC} + K_{SAN}^{WT} \frac{\mu_2}{s_2} m_{SAN,DDC} E[X_{2,DDC}] \mu_1 P_{est}^{12,DDC} \\ &= K_{SAN}^{WT} \mu_1 \mu_2 m \frac{N_{DDC}}{N_{TOT}} \left(1 - \frac{1}{R_{WT}(1-s_1)(1-s_2)}\right) \\ &\quad \times \left[\frac{1}{s_1}\left(\frac{R_{WT}(1-s_1)(1-\epsilon_2)}{1-R_{WT}(1-s_1)(1-\epsilon_2)}\right) + \frac{1}{s_2}\left(\frac{R_{WT}(1-s_2)(1-\epsilon_1)}{1-R_{WT}(1-s_2)(1-\epsilon_1)}\right)\right] \end{aligned} \tag{26}$$

Migration-mutation-mutation path In this path a wild-type migrant from the sanctuary goes to the double-drug compartment, where it gains both mutations. The rate at which this path happens is proportional to the carrying capacity of the wild-type population in the sanctuary (the number of

infected cells at equilibrium), the migration rate, the size of the wild-type infection in the double-drug compartment before going extinct, both mutation rates, and the establishment probability of the double mutant in the double-drug compartment. Mutations can occur in either order.

$$\begin{aligned} r_{02}^{m\mu\mu} &= K_{SAN}^{WT} m_{SAN,DDC} E[X_{WT,DDC}] \mu_1 E[X_{1,DDC}] \mu_2 P_{est}^{12,DDC} \\ &\quad + K_{SAN}^{WT} m_{SAN,DDC} E[X_{WT,DDC}] \mu_2 E[X_{2,DDC}] \mu_1 P_{est}^{12,DDC} \\ &= K_{SAN}^{WT} \mu_1 \mu_2 m \frac{N_{DDC}}{N_{TOT}} \left(\frac{R_{WT}(1-\epsilon_1)(1-\epsilon_2)}{1-R_{WT}(1-\epsilon_1)(1-\epsilon_2)} \right) \left(1 - \frac{1}{R_{WT}(1-s_1)(1-s_2)} \right) \\ &\quad \times \left[\left(\frac{R_{WT}(1-s_1)(1-\epsilon_2)}{1-R_{WT}(1-s_1)(1-\epsilon_2)} \right) + \left(\frac{R_{WT}(1-s_2)(1-\epsilon_1)}{1-R_{WT}(1-s_2)(1-\epsilon_1)} \right) \right] \end{aligned} \tag{27}$$

Comparison The total rate of colonization is $r_{02} = r_{02}^{\mu\mu m} + r_{02}^{\mu m\mu} + r_{02}^{m\mu\mu}$. For most of the parameter ranges we will consider, the rate of the mutation-mutation-migration path is much larger than the rate of the migration-mutation-mutation or mutation-migration-mutation path. This is because we consider the cost of the mutations (s_1, s_2) to be relatively small but the drug efficacy to be quite large $(\epsilon_1, \epsilon_2 \approx 1)$, so that the fitness of the mutant in the sanctuary is much larger than the fitness of the wild type in the single or double-drug compartments.

6 Modified rate equations to account for temporal clustering of mutations

We found that the rate expressions used above in the simplified Markov process did a very good job of qualitatively explaining our simulation results, but consistently over-estimated the rate of treatment failure, especially at low mutation rates, high migration rates, and low costs of resistance. Through extensive simulations, we determined that this was due to an approximation inherent in the rate formulas presented in Sections 5.1, 5.2 and 5.3. Because the mutation-migration (or mutation-mutation-migration) path is dominant for all parameter ranges relevant to our study, we focus on describing the issue and correction for this rate.

Equations (21), (24) and (25) assume that mutants (e.g. single mutants in the sanctuary in Eq. (21)) are present at their expected mutation-selection frequency given by Eqs. (12) and (17) at all times. However, in some parts of parameter space, this deterministic approximation leads to a drastic overestimation of the rate of evolution of drug resistance. This overestimate occurs because in reality, the prevalence of mutants varies in such a way that mutants tend to "clump" together temporally. When the total rate of generating single mutants in a compartment is low ($K\mu << 1$), but mutations are not very costly ($s << 1$), then mutants may not be present in the population in most generations, but when they are present, then subcritical but efficient replication may cause them to exist at frequencies much higher than the mutation-selection balance prediction. If, in addition, the eventual probability of migrating and fixing in one of the other compartments is fairly

high for each mutated individual, then the approximations of §5.1-5.3 will be far off, because the probability that at least one of a group of mutants is successful will be a highly non-linear function of the number of mutants. Using the average (or expected) number of mutants will therefore overestimate the rate of adaptation. See Figure S4 for an example of a parameter region where there is less temporal clumping of mutations and migration rates are higher so the simplified Markov process has a much better agreement with the stochastic simulations.

Intuitively, this can be understood as follows. Suppose the expected number of mutations existing in a particular compartment is 1, and each mutant individiual individual has a 10% probability of migrating and establishing in the next compartment. We can demonstrate that adaptation will occur faster if 1 mutant is consistently generated every generation, as opposed to 100 mutants all occuring in one generation, every hundred generations. In the former case, there is overall a 10% change of successful invasion every generation, leading to an expected waiting time for success of 10 generations. In the latter case, there is an $\sim$ 100% chance of succsesful invasion every hundredth generation, leading to an expected waiting time for success of 100 generations. In this case, for a pathogen population trying to adapt, it would be much better to have 1 mutant every generation (assuming expected number of mutants is 1) that has a 10% probability of success, than to have 100 mutants all occurring in one generation, once in a hundred generations even though success is virtually guaranteed in this generation.

Previous work has demonstrated that this effect is important for tunnelling (11) and also for adaptation from standing genetic variation (Fig. 2 of Hermisson and Pennings(12)). Here we adapt the mathematical approach of Weissman et al. (Appendix C) to recalcuate Equations (21), (24) and (25), taking into account this uneven temporal distribution of mutations. We can avoid needing to exactly specify this distribution by instead using a *first-step analysis*, which considers each event that can happen to a single mutant individual and uses this to implicitly calculate the ultimate probability of reaching and establishing infection in a new compartment.

6.1 Colonization of the single-drug compartment by single resistant mutants

We consider first the rate at which the single-drug compartment (SDC) is colonized by single resistant mutants originating in the sanctuary (SAN). We focus on the mutation-migration path, as it is dominant for the entire parameter range of interest in this paper (drug treatment is highly efficacious and mutations have a low fitness cost).

The previous approach involved separately calculating and then multiplying together i) the expected number of secondary mutants generated from each mutation event from the wild type, ii) the probability that each will migrate, and iii) the establishment; instead, this approach calculates this entire process together. We call the overall probability that any single mutant (strain "1", directly resulting from a mutational event or one of its offspring) will migrate from the SAN to the SDC and establish the "rescue probability", $p_{resc}^{1,SAN,SDC}$. Once we know this probability, then the overall

rate of generating single drug resistance is the product of this number and the rate of mutational events from the wild type.

The first-step analysis uses the fact that the the rescue probability for an individual mutant is equal to the probability that this individual itself establishes or that it produces an offspring that establishes. There are four possible first events that can occur to an individual:

- With rate $m_{SAN,SDC}$, it can migrate to the SDC, resulting in rescue with probability $P_{est}^{1,SDC}$
- With rate d_y, it can die, resulting in zero probability of rescue
- With rate $m_{SAN,o} - m_{SAN,SDC}$, it can migrate to another compartment, resulting in zero probability of rescue
- With rate $(d_y + m_{SAN,o})(1 - s_1)$, it can replicate and produce two identical mutant individuals, and the probability that at least one of them is successful is $1 - (1 - p_{resc}^{1,SAN,SDC})^2$.

Here $m_{SAN,o} = \sum_{j \neq SAN} m_{SAN,j}$ is the migration rate to any compartment outside the sanctuary. We also use the fact that the turnover rate of the wild-type population in the SAN at equilibrium is the sum of the death rate (d_y) and the outward migration rate $m_{SAN,o}$, because at equilibrium, input to compartment must equal output from compartment. The replicate rate of the mutant population is reduced by a factor of $1 - s$ compared to the wild type. Because we are using rates rather than probabilities, we can normalize by the sum of the rates to get the expression

$$p_{resc}^{1,SAN,SDC} = \frac{m_{SAN,SDC} P_{est}^{1,SDC} + dy \cdot 0 + (m_{SAN,o} - m_{SAN,SDC}) \cdot 0}{(dy + m_{SAN,o})(2 - s_1)} + \frac{(dy + m_{SAN,o})(1 - s_1)(1 - (1 - p_{resc}^{1,SAN,SDC})^2)}{(dy + m_{SAN,o})(2 - s_1)} \quad (28)$$

This equation can be solved for $p_{resc}^{1,SAN,SDC}$ to give

$$p_{resc}^{1,SAN,SDC} = \frac{-s_1 + \sqrt{s_1^2 + 4(1 - s_1) m_{SAN,SDC} P_{est}^{1,SDC} / (dy + m_{SAN,o})}}{2(1 - s_1)} \quad (29)$$

To calculate the overall rate of this path, $r_{01}^{\mu m}$ we need the rate of mutational events. This is the product of the number of cells turning over each day (the carrying capacity of the SAN, K_{SAN}^{WT} multiplied by the turnover rate) and the mutation rate, u_1. As a result, the rate of invasion of the SDC from the SAN becomes

$$r_{01} \approx r_{01}^{\mu m} = K_{SAN}^{WT} (dy + m_{SAN,o}) \mu_1 p_{resc}^{1,SAN,SDC} \quad (30)$$

6.2 Colonization of the double-drug compartment via the single-drug compartment

Using the same method as above, we get the probability that a mutational event that produces a double mutant (strain "12") in the SDC leads to successful invation of the DDC

$$p_{resc}^{12,SDC,DDC} = \frac{-s_2 + \sqrt{s_2^2 + 4(1-s_2)m_{SDC,DDC}P_{est}^{12,DDC}/(dy + m_{SDC,o})}}{2(1-s_2)} \tag{31}$$

where in this case $m_{SDC,o} = \sum_{j \neq SDC} m_{SDC,j}$, so that

$$r_{12} \approx r_{12}^{\mu m} = K_{SDC}^{1}(dy + m_{SDC,o})\mu_2 p_{resc}^{12,SDC,DDC} \tag{32}$$

6.3 Colonization of the double-drug compartment directly from the sanctuary

We next determine the rate at which the the double-drug compartment (DDC) is colonized by double resistant mutants originating in the sanctuary (SAN). We focus on the mutation-mutation-migration path, for the same reasons discussed above. Because this process involves three steps, we will need to invoke the first-step analysis twice. First, we will need to determine the overall probability that any single mutant (strain "1", directly resulting from a mutational event or one of its offspring) will gain a second mutation and migrate from the SAN to the DDC. We call this rescue probability $p_{resc}^{1,SAN,DDC}$. However, this rescue probability will depend on the probability that any double mutant (strain "12", directly resulting from a mutational event or one of its offspring) will migrate from the SAN to the DDC, $p_{resc}^{12,SAN,DDC}$.

We consider first the probability of rescue starting from a single mutant resistant to drug 1, $p_{resc}^{1,SAN,DDC}$. For a single mutant individual in the SAN, there are four possible first events that can occur:

- With rate $m_{SAN,o}$, it can migrate away, resulting in zero probability of rescue
- With rate d_y, it can die, resulting in zero probability of rescue
- With rate $(d_y + m_{SAN,o})(1-s_1)u_2$, it can replicate and produce one double mutant offspring, and the probability that either the single or double mutant is successful is $p_{resc}^{1,SAN,DDC} + p_{resc}^{12,SAN,DDC}(1 - p_{resc}^{1,SAN,DDC})$.
- With rate $(d_y + m_{SAN,o})(1-s_1)(1-u_2)$, it can replicate without mutating, and the probability that at least one of the resulting single mutants is successful is $1 - (1 - p_{resc}^{1,SAN,DDC})^2$.

We can write the rescue probability as the sum of the probabilities of each first-step event multiplied by probability of rescue conditional upon this first step to get

$$p_{resc}^{1,SAN,DDC} = \frac{m_{SAN,o} \cdot 0 + dy \cdot 0 + (dy + m_{SAN,o})(1 - s_1)u_2(p_{resc}^{1,SAN,DDC} + p_{resc}^{12,SAN,DDC}(1 - p_{resc}^{1,SAN,DDC}))}{(dy + m_{SAN,o})(2 - s_1)} + \frac{(dy + m_{SAN,o})(1 - s_1)(1 - u_2)(1 - (1 - p_{resc}^{1,SAN,DDC})^2)}{(dy + m_{SAN,o})(2 - s_1)} \quad (33)$$

which, when solved for $p_{resc}^{1,SAN,DDC}$, gives:

$$p_{resc}^{1,SAN,DDC} = \frac{-(s_1 + (1 - s_1)u_2(p_{resc}^{12,SAN,DDC} + 1))}{2(1 - s_1)(1 - u_2)} + \frac{\sqrt{(s_1 + (1 - s_2)u_2(p_{resc}^{12,SAN,DDC} + 1))^2 + 4(1 - s_1)^2 u_2(1 - u_2)p_{resc}^{12,SAN,DDC}}}{2(1 - s_1)(1 - u_2)} \quad (34)$$

Rescue could also occur starting from a single mutant resistant instead to drug 2, with a probability $p_{resc}^{2,SAN,DDC}$, which by symmetry is given by

$$p_{resc}^{2,SAN,DDC} = \frac{-(s_2 + (1 - s_2)u_1(p_{resc}^{12,SAN,DDC} + 1))}{2(1 - s_2)(1 - u_1)} + \frac{\sqrt{(s_2 + (1 - s_1)u_2(p_{resc}^{12,SAN,DDC} + 1))^2 + 4(1 - s_2)^2 u_1(1 - u_1)p_{resc}^{12,SAN,DDC}}}{2(1 - s_2)(1 - u_1)} \quad (35)$$

These formulae require knowing $p_{resc}^{12,SAN,DDC}$, which can be calculated using a separate first-step analysis that considers each possible first even that can occur to a double mutant in the sanctuary:

- With rate $m_{SAN,DDC}$, it can migrate to the DDC, resulting in rescue with probability $P_{est}^{12,DDC}$
- With rate d_y, it can die, resulting in zero probability of rescue
- With rate $m_{SAN,o} - m_{SAN,DDC}$, it can migrate to another compartment, resulting in zero probability of rescue
- With rate $(d_y + m_{SAN,o})(1 - s_1)(1 - s_2)$, it can replicate and produce two identical double mutant individuals, and the probability that at least one of them is successful is $1 - (1 - p_{resc}^{12,SAN,DDC})^2$.

This gives us the implicit formula for $p_{resc}^{12,SAN,DDC}$

$$p_{resc}^{12,SAN,DDC} = \frac{m_{SAN,DDC}P_{est}^{12,DDC} + dy \cdot 0 + (m_o - m_{SAN,DDC}) \cdot 0}{(dy + m_{SAN,o})(1 + (1 - s_1)(1 - s_2))} + \frac{(dy + m_{SAN,o})(1 - s_1)(1 - s_2)(1 - (1 - p_{resc}^{12,SAN,DDC})^2)}{(dy + m_{SAN,o})(1 + (1 - s_1)(1 - s_2))} \quad (36)$$

which can be solved to give

$$p_{resc}^{12,SAN,DDC} = -\frac{(1-(1-s_1)(1-s_2))}{2(1-s_1)(1-s_2)} + \frac{\sqrt{(1-(1-s_1)(1-s_2))^2 + 4(1-s_1)(1-s_2)m_{SAN,DDC}P_{est}^{12,DDC}/(dy+m_{SAN,o})}}{2(1-s_1)(1-s_2)}. \quad (37)$$

The overall rate of this path of invasion of the DDC from the SAN, $r_{02}^{\mu\mu m}$, which includes the fact that mutations may occur simultaneously or in either order, is then

$$r_{02} \approx r_{02}^{\mu\mu m} = K_{SAN}^{WT}(dy + m_{SAN,o})(\mu_1 p_{resc}^{1,SAN,DDC} + \mu_2 p_{resc}^{2,SAN,DDC} + \mu_1\mu_2 p_{resc}^{12,SAN,DDC}). \quad (38)$$

6.4 Limiting forms

In particular limits, these modified equations reduce to the expression given in Sections 5.1 - 5.3. By comparing the expressions for $r_{01}^{\mu m}$ and $r_{12}^{\mu m}$ in Equations (30) and (32) to those in (21) and (24), we see that these are equivalent in the limit that $(1-s)p_{mig,est}/s^2 \ll 1$. Here $p_{mig,est}$ is the probability that an individual mutant will migrate to the target compartment before dying or migrating to another compartment. For example, for colonization of the SDC, $p_{mig,est} = m_{SAN,SDC}P_{est}^{1,SDC}/(d_y + m_{SAN,o})$. In this limit, the probability that at least one individual in the lineage of the mutant produced from the wildtype is able to establish infection in a new compartment can be well-approximated by the product of the average lineage size ($1/s$) and the migration-establishment probability ($p_{mig,est}$). Note that this limit does not depend on μ. For the direct path, the conditions that lead to equivalence between $r_{02}^{\mu\mu m}$ given by (38) and (25) are more climplicated, and do depend on μ.

7 Comparison of stepwise versus direct path to acquired double-drug resistance

One way to quantify the influence of single drugs compartments (SDC) on the evolution of drug resistance is to determine the compartment size at which the probability of stepwise evolution becomes equal to the probability of direct evolution in the absence of this compartment. This corresponds to the "crossing point" of the two lines in Fig 2. If the probabilities become equal when the SDC are small relative to the double-drug compartments, this indicates that this extra compartment has a disproportionate influence on the risk of resistance.

Because the analytic calculations described in the previous sections match extremely well with the simulation results (Fig 2 and Fig S4), we can numerically predict the SDC size at the cross point by setting the conditional cumulative distribution functions for the probability of treatment failure (Equation 19) by the direct ($F_{02}(t)$) or stepwise ($F_{012}(t)$) path equal, and solving for N_{SDC}/N_{DDC}. However, we would like to have an expression for this value, to understand its dependence on

the parameter values. While no general closed form solution exists, we can get an approximate expression in two different regimes.

For both regimes we use the simpler expressions given in Section 5, which although neglecting temporal clustering of mutants, only slightly overestimates rates of evolution for the parameter ranges we use, and yields much more comprehensible formulae.

Approximation 1 The first approximation is valid if we look at treatment outcomes when a short enough time (t) has passed so that the prevalence of either single drug resistance or treatment failure is low and all steps are rate-limited ($r_{01}t \ll 1$, $r_{12}t \ll 1$, $r_{02}t \ll 1$). This situation occurs for the results presented in Fig 2a. In this limit,

$$\begin{aligned} F_{02}(t) &\approx r_{02}t \\ &\approx K_{SAN}^{WT}\frac{\mu^2}{s^2}\left(m\frac{N_{DDC}}{N_{TOT}}\right)\left(1-\frac{1}{R_{WT}(1-s)^2}\right)t \\ F_{012}(t) &\approx \frac{1}{2}r_{01}r_{12}t^2 \\ &\approx \frac{1}{2}K_{SAN}^{WT}\frac{\mu}{s}\left(m\frac{N_{SDC}}{N_{TOT}}\right)\left(1-\frac{1}{R_{WT}(1-s)}\right)K_{SDC}^{1}\frac{\mu}{s}\left(m\frac{N_{DDC}}{N_{TOT}}\right)\left(1-\frac{1}{R_{WT}(1-s)^2}\right)t^2 \end{aligned} \tag{39}$$

Setting $F_{02}(t) = F_{012}(t)$, and using the definitions of the carrying capacities (Equation 3), we find that the cross-point occurs when

$$\frac{N_{SDC}}{N_{DDC}} \approx \frac{N_{SDC}}{N_{TOT}} = \left(\frac{1}{2}mN_{TOT}\frac{d_x}{d_y}\left(1-\frac{1}{R_{WT}(1-s)}\right)^2 t\right)^{(-1/2)}. \tag{40}$$

We use the fact that the double-drug compartment comprises the vast majority of the body for all situations we study. Therefore, in this limit, the size of the SDC where the stepwise path to resistance becomes more important than the direct path increases with the pathogen virulence (d_y/d_x), but decreases with the migration rate (m), the total number of uninfected cells before treatment (N_{TOT}, the time of observation (t), and (weakly) with the fitness of the single mutant ($R_{WT}(1-s)$)

Approximation 2 A second approximation may hold for longer times, if the system is in a regime where treatment time is long enough so that most individuals who developed single drug resistance progressed to treatment failure ($r_{12}t \gg 1$), but the other (generally slower) steps remain rate limiting ($r_{01}t \ll 1, r_{02}t \ll 1$. This situation occurs for the results presented in Fig 2b. In this limit,

$$\begin{aligned} F_{02}(t) &\approx r_{02}t \\ &\approx K_{SAN}^{WT}\frac{\mu^2}{s^2}\left(m\frac{N_{DDC}}{N_{TOT}}\right)\left(1-\frac{1}{R_{WT}(1-s)^2}\right)t \\ F_{012}(t) &\approx r_{01}t \\ &\approx K_{SAN}^{WT}\frac{\mu}{s}\left(m\frac{N_{SDC}}{N_{TOT}}\right)\left(1-\frac{1}{R_{WT}(1-s)}\right)t \end{aligned} \tag{41}$$

Setting $F_{02}(t) = F_{012}(t)$, we find that the cross-point occurs when

$$\frac{N_{SDC}}{N_{DDC}} = \frac{u}{s}\left(1 - \frac{1}{R_{WT}(1-s)^2}\right)\left(1 - \frac{1}{R_{WT}(1-s)}\right)^{-1} \approx \frac{u}{s}. \tag{42}$$

We use the fact that the cost of resistance is small ($s \ll 1$) and $R_{WT}(1-s)^2 > 1$. This simpler and more intuitive result demonstrates that the more infrequently mutations occur and the more costly they are, the rarer it is to get double mutants, and the more important the stepwise path involving the SDC is.

Note that for many parameter values and treatment times, neither of these approximations may be appropriate.

8 Including pre-existing resistance

For the main results of the paper, we ignore the effects of pre-existing single or double resistance mutations in compartments containing one or both drugs. However, we present simulation results including this standing genetic variation in Figure 3. Here we present calculations for the probability of pre-existing mutations, and with these expressions and formulation of Section 4.2, we can analytically calculate how standing genetic variation changes the rate of acquiring resistance with and without single-drug compartments.

8.1 Probability of pre-existing single drug resistance in the single-drug compartment

There are two mechanisms by which single drug resistance mutations may colonize the single-drug compartment (SDC) very shortly after treatment begins, without being generated by the sanctuary. When drug treatment starts, there is an existing wild-type infection in all compartments. In the SDC, this infection has a size K_{SDC}^{WT}. A mutation can either exist at mutation-selection balance in this initial population, or, if the drug is not 100% efficacious, it can arise during replication that continues as the wild-type population decays in the presence of the drug.

The relative probabilities of these two paths were considered in an early viral dynamics paper (13), and they found that the probability of pre-existing mutation is always greater than the probability of a newly generated mutation (assuming that the drug treatment results can suppress the wild-type population, i.e. $R_{WT}(1-\epsilon_1) < 1$). They only used deterministic results, and did not consider establishment probabilities. Newer work presented by Alexander and Bonhoeffer(9) revisited this questions through a stochastic viral dynamics framework, and finds more nuanced results - the relative important of *de novo* mutations depends on many parameters of the model - including s, ϵ, d_y/d_x and R_{WT}. Lower drug efficacies and higher costs of the mutation tend to make the contributions of *de novo* mutations greater than pre-existing mutations. Here we summarize the derivations of Alexander and Bonhoeffer as they apply to our system.

Time-dependent establishment probability For both pre-existing and *de novo* single drug mutations arising in the single-drug compartment, we will need to know the establishment probability. When $R_{WT}(1-\epsilon_1) < 1$, which we assume throughout the paper, the wild-type infection in the SDC decays approximately exponentially as uninfected cells recover. The equations describing the dynamics for uninfected cells $x(t)$ and infected cells $y(t)$ are (9)

$$\begin{aligned} x(t) &\approx N_{SDC}(1-(1-1/R_{WT})e^{-d_x t}) \\ y(t) &\approx K_{SDC}^{WT} e^{(g_1(0,s)(e^{-d_x t}-1)+g_2(s)d_x t)} \end{aligned} \tag{43}$$

with the functions g_1 and g_2 given by

$$\begin{aligned} g_1(t,s) &= d_y/d_x e^{-d_x t}(R_{WT}-1)(1-s) \\ g_2(s) &= d_y/d_x(R_{WT}(1-s)-1) \end{aligned} \tag{44}$$

Because the number of available target cells depends on time, so does the effective R_0 of the invading mutant ($R_0^{1,SDC}(t) = R_{WT}(1-s)x(t)/N_{SDC}$) and therefore the establishment probability, $P_{est}^{1,SDC} = 1 - 1/R_0^{1,SDC}$ (§2). Initially, the establishment probability is zero (because $x(0) = N_{SDC}/R_{WT}$ and so $R_0^{1,SDC}(0) = 1-s < 1$), and it increases over time. Alexander and Bonhoeffer(9) derive an expression for $P_{est}^{1,SDC}(t)$ for a mutant that appears at time t,

$$P_{est}^{1,SDC}(t) = \left(1 + \frac{d_y}{d_x} e^{g_1(t,s)} g_1(t,s)^{-g_2(s)} \Gamma(g_2(s), 0, g_1(t,s))\right)^{-1} \tag{45}$$

where the generalized incomplete Gamma function is $\Gamma(z, a_1, a_2) = \int_{a_1}^{a_2} x^{z-1}e^{-x}dx$. Note that $P_{est}^{1,SDC}(t) \neq 0$. Here t refers to the time a mutant appears, not the time at which it establishes, and since each strain has an average lifespan of $1/d_y$ days, it may establish towards the end of its life when infected cell levels have recovered enough that $R_0^{1,SDC} > 0$.

Mutation pre-exists in wild-type population The wild-type population that is initially present in the single-drug compartment before drug treatment may harbor a resistance mutation. As shown in §3.1, the probability generating function for the distribution of the initial single mutant population size is

$$F(z) = \left(\frac{s_1}{1-(1-s_1)z}\right)^{\left(\frac{K_{SDC}^{WT}\mu}{(1-s_1)}\right)}$$

where the probability that there are n mutants can be recovered as $p(n) = \frac{1}{n!}\frac{d^n F}{dz^n}|_{z=0}$, and the average number of mutants is $E[z] = \frac{dF}{dz}|_{z=1} = K_{SDC}^{WT}\mu/s$. The establishment probability of each of these mutants is $P_{est}^{1,SDC}(0)$ (Eq. (45)), and so the overall probability that at least one mutant

establishes an infection is

$$\begin{aligned} p &= \sum_{n=0}^{\infty} p(n)(1-(1-P_{est}^{1,SDC}(0))^n) \\ &= 1 - F(1-P_{est}^{1,SDC}(0)) \\ &= 1 - \left(\frac{s}{1-(1-s)(1-P_{est}^{1,SDC}(0))}\right)^{\left(\frac{K_{SDC}^{WT}\mu}{(1-s)}\right)} \end{aligned} \tag{46}$$

Mutation arises *de novo* from the wild type The wild-type population that is initially present in the single-drug compartment before treatment begins can generate a new resistance mutation during the period when the drug is first administered and the wild-type population is declining. The probability that a new mutation is generated during this decay depends on the product of the rate of new mutations generated and their establishment probability, which are both are time-dependent quantities(9). This product is given by

$$r(t) = K_{SDC}^{WT} d_y R_{WT}(1-\epsilon)\mu \left(1-\left(1-\frac{1}{R_{WT}}\right)e^{-d_x t}\right) e^{(g_1(0,s)(e^{-d_x t}-1)+g_2(s)d_x t)} P_{est}^{1,SDC}(t) \tag{47}$$

where g_1 and g_2 are the same as defined in Equation (44). From $r(t)$, the total probability that a *de novo* mutation single mutant arises in the SDC and establishes is

$$p = 1 - e^{-\int_0^\infty r(t)dt} \tag{48}$$

Comparison The total probability of single mutants establishing in the SDC shortly after treatment initiation, due to standing genetic variation (p_{ss}), is the sum of these two probabilities. When the cost of the mutation is relatively small ($s \ll 1$) but the drug efficacy is quite high ($\epsilon \approx 1$), the chance that these mutants arise from mutation-selection balance is much higher than the chance that they arise *de novo* during drug decay. We tested this for the range of parameter values used in the main text figures.

8.2 Probability of pre-existing double drug resistance in the double-drug compartment

There are three ways to develop resistance in the double-drug compartment that do not involve the other compartments at all. When drug treatment starts, there is an existing wild-type infection in the double-drug compartment. A double mutation can either exist at mutation-selection balance in this initial population, or, if the drug is not 100% efficacious, it can arise during replication that continues as the wild-type population, or pre-existing single resistant mutants, decays in the presence of the drug. Due to our findings (above) that the first path is much more important for single mutations in the SDC, we assume the same is true for double mutants in the DDC, and only present this calculation. The agreement of these approximations with the full simulation results validates this approach

Double resistant mutant pre-exists in wild-type population As described in §3.2, we can approximate the distribution of the number of pre-existing double mutants, and hence the probability that at least one establishes an infection. Using Equation 16, the probability that at least one pre-existing double resistant mutant establishes an infection is

$$p = 1 - \left(\frac{1-(1-s_1)(1-s_2)}{1-(1-s_1)(1-s_2)(1-P_{est}^{12,DDC}(0))} \right)^{K_{DDC}^{WT} \frac{\mu_1 \mu_2}{s_1 s_2}} \tag{49}$$

where $P_{est}^{12,DDC}(0)$ follows the same form as Eq. (45) except that s_1 is replaced with $1-(1-s_1)(1-s_2)$.

We therefore approximate this rate p as the total probability of double mutants establishing shortly after treatment initiation in the DDC, p_{dd}.

Part III
Simulations

9 Overview

We developed a fully stochastic simulation where we keep track of the genotype and location of every infected cell in the body. We explicitly simulate all the events that might occur to an infected cell: replication (representing either division of a bacterial cell or infection of a new cell by a virus), mutation (upon replication), migration and death. Events are chosen with a probability that is proportional to their rate of occurrence. Once an event is executed, time is updated using the total rate of all the possible events that could have occurred. This method for exact stochastic simulation of Poisson processes is known as the Gillespie algorithm.

Rates of replication, death and migration The replication rate of cells of type i in compartment j, $r_{ij}^{replication}$, and the death rate r_{ij}^{death}, are calculated using the deterministic basic viral dynamics model described above (§1). To speed up the simulation of large numbers of cells over long time periods, which we must repeat thousands of times, the model can be additionally simplified to a single equation for the dynamics of infected cells. This is accomplished by assuming that uninfected cells numbers change in parallel to infected cell numbers, without any lags, by setting $\dot{x} = 0$. We then get a reduced model

$$\dot{y_{ij}} = \left[\frac{\lambda_j d_y R_0^{ij}}{\lambda_j + \sum_{l=1}^{n} R_0^{lj} d_y y_{lj}} \right] y_{ij} - d_y y_{ij} \tag{50}$$

where the first term gives $r_{ij}^{replication}$ and the second term tells us that $r_{ij}^{death} = d_y$ for all i, j. The rate of production of uninfected cells in our model is $\lambda_j = N_j d_x$. This approximation in general has very little effect on our results, as lags in target cell recovery or decline matter most when

the total viral population size is changing rapidly in a compartment, which occurs on a timescale much shorter than the evolutionary processes we are interested in. We have validated this using a full simulation tracking infected as well as uninfected cells. However, this lag can influence the fixation probability of pre-existing mutations in drug-treated compartments (§8), and so this approximation was not used for results including standing genetic variation.

The rate of migration out of a compartment does not depend on the type of the cell, so the total outward migration rate is $r_{ij}^{migration} = \sum_{k=0}^{3} m_{jk}$ for all i. As in the main text, m_{jk} is the migration rate from compartment j to compartment k.

10 Simulation algorithm

1. **Calculate the rate of every possible event**
   We denote the rate of an event as α_{ijk} where $i = \{0, 1, 2, 3\}$ corresponds to the genotype of the cell to which the event will occur (wild type, single mutant 1, single mutant 2, double mutant), $j = \{0, 1, 2, 3\}$ corresponds to the compartment where the event will occur (SAN, SDC1, SDC2, DDC) and $k = \{0, 1, 2\}$ corresponds to the type of event (replication,death, migration). We can write $\alpha_{ijk} = n_{ij} r_{ijk}$, where n_{ij} is the number of cells of type i in compartment j and r_{ijk} is the rate at which event k occurs for cells of type i in compartment j. If $k = 0$, $r_{ijk} = r_{ij}^{replication}$, if $k = 1$, $r_{ijk} = r_{ij}^{death}$ and if $k = 2$, $r_{ijk} = r_{ij}^{migration}$. The total rate of possible events that can occur is $\alpha_T = \sum_i \sum_j \sum_k \alpha_{ijk}$.

2. **Determine which event will occur next**
   Draw a random number X from $[0, 1]$. If $X\alpha_T < \alpha_{000}$ the next event will be replication of one wild-type strain in the sanctuary, if $\alpha_{000} < X\alpha_T < \alpha_{000} + \alpha_{001}$, the next event will be death of one wild-type strain in the sanctuary and so on for all the 48 possibilities. We will denote the genotype and compartment of the cell where next event will occur as i' and j' respectively.

3. **Execute event**

   (a) Replication. Draw an additional random number from $(0, 1)$ to determine if the cell mutates to any of the other three genotypes or remains of type i'. Only one mutation event per drug can occur. Increase the number of cells of the type chosen after mutation in compartment j' by 1.

   (b) Death. Decrease the number of cells of type i' in compartment j' by 1.

   (c) Migration. Draw an additional random number from $(0, 1)$ to determine where the cell migrates. Decrease the number of cells of type i' in compartment j' by 1 and increase its number in the target compartment by 1.

4. **Update time** Update the time from t to $t + \tau$ where τ is a number randomly drawn from an exponential distribution with mean $\frac{1}{\alpha_T}$.

These steps are iterated until a maximum time is reached (for Figures 2a, 2b) or until there is colonization of the double-drug compartment (for Figures 2c, 2d, 3 and 4). We assume that the double-drug compartment is colonized and consequently treatments fails if there are more than 10 double-drug resistant mutants in the double-drug compartment. We chose this threshold since the probability that a population of 10 double-drug resistant mutants goes extinct in the double-drug compartment is of the order of 10^{-6} for the parameter values that we use in our simulations.

For results including standing genetic variation we additionaly keep track of the genotype and location of every uninfected cell in the body and explicitly simulate all the events that might occur to both infected and uninfected cells: replication of uninfected cells, infection, mutation upon infection, death of both uninfected and infected cells, and migration of infected cells among different compartments. If treatment does not fail and the number of uninfected cells in the double-drug compartment is restored to the value at carrying capacity by the action of the drug then we switch to simulating only the dynamics of infected cells.

10.1 Initial conditions

10.1.1 Not including standing genetic variation

We assume that when treatment starts the wild-type population is at its carrying capacity in the sanctuary and the other compartments have no infected cells. Thus, the initial number of wild-type strains in the sanctuary is K_{SAN}^{WT}. We also assume that the population is at mutation-selection equilibrium in the sanctuary so we sample the initial number of mutants resistant to drug 1, the initial number of mutants resistant to drug 2 and the initial number of double-drug resistant mutants from Poisson distributions with means $K_{SAN}^{WT}\frac{\mu_1}{s_1}$, $K_{SAN}^{WT}\frac{\mu_2}{s_2}$ and $K_{SAN}^{WT}\frac{\mu_1\mu_2}{s_1 s_2}$ respectively.

10.1.2 Including standing genetic variation

We account for pre-existing mutations by simulating the infection before initiating treatment. We assume that the wild-type starts at its carrying capacity in all the four compartments and simulate the infection for 100 days (since there are no drugs, the R_0 of the wild-type is R_{WT} in all the compartments). We verified that this time is long enough for the population of infected cells to reach mutation-selection balance in all the compartments before treatments starts.

11 Distinguishing paths to resistance evolution in simulations

We distinguish between the direct and the stepwise path to resistance evolution by determining whether the single-drug compartment is already colonized by single-drug resistant mutants when treatment fails. We assume that the single-drug compartment is colonized if it has more than 10 single-drug resistant mutants. We chose this threshold since the probability that a population of 10 single-drug resistant mutants goes extinct in the single-drug compartment is of the order of 10^{-6} for the parameter values that we use in our simulations. When there is more than one single-drug compartment, stepwise evolution of resistance can happen via three different paths: Either of the

single-drug compartments can be colonized before the double-drug compartment or both single-drug compartments can be colonized before the double-drug compartment. We study the relative frequency of the stepwise paths to resistance evolution in Figure 4.

12 Determining the average viral load

The mean viral load is the average of the total number of infected cells over all the time steps in the simulation weighted by the length of each time step. This is $(\sum_i V_i \tau_i)/t_{total}$, where V_i is the total number of infected cells in time step i, τ_i is the length of time step i and $t_{total} = \sum_i \tau_i$ is the total simulation time.

13 Information on figures in the main text

The following parameter values are the same in all figures: $R_{WT} = 4, \epsilon_1 = 0.99, \epsilon_2 = 0.99, d_y = 1$ d^{-1}, $d_x = 0.1$ d^{-1} and $m = 0.1$ d^{-1}.

Figure 2

Figures 2a and 2b

The infection is simulated until the total time has been reached regardless of whether treatment failed or not. The size of the compartment with drug 1, N_{SDC1}, increases along the x-axis and each point is the fraction of the total number of simulated patients that failed via the indicated path (either direct or stepwise). For each value of N_{SDC1} treatment has failed in at least 2000 simulated patients.

Parameters: $s_1 = 0.05, s_2 = 0.05, \mu_1 = 10^{-5}, \mu_2 = 10^{-5}, N_{SAN} = 10^5$ cells, $N_{SDC2} = 0$ cells, $N_{DDC} = 10^7$ cells, Total time: 365 days (Figure 2a), Total time: 3650 days (Figure 2b).

Figures 2c and 2d

We show an example run of a simulated patient where the double-drug compartment is colonized in the absence (Figure 2c) and the presence (Figure 2d) of a single-drug compartment containing drug 1. The mean time to treatment failure over 2000 simulated patients for the parameters in Figure 2c is 1.576×10^5 days and for the parmeters in Figure 2d is 2270 days.

Parameters: $s_1 = 0.05, s_2 = 0.05, \mu_1 = 10^{-5}, \mu_2 = 10^{-5}, N_{SAN} = 10^5$ cells, $N_{SDC2} = 0$ cells, $N_{DDC} = 10^7$ cells, $N_{SDC1} = 0$ cells (Figure 2c), $N_{SDC1} = 5 \times 10^4$ cells (Figure 2d).

Figure 3

We simulate the infection until there is colonization of the double-drug compartment. To capture the trade-off between total drug coverage and the presence of a single-drug compartment, the size of the single-drug compartment with drug 1 increases along the x-axis keeping $N_{SAN}+N_{SDC1}$ constant. We plot both the mean viral load until treatment failure and the fold-increase in the adaptation rate relative to the case when there are no single-drug compartments ($N_{SAN} = 10^5$ cells, $N_{SDC1} = 0$ cells). The adaptation rate is calculated as $\frac{1}{T_f}$ where T_f is the average time to treatment failure over at least 30000 simulations. The fold-increase in adaptation rate relative to $N_{SDC1} = 0$ is shown both for simulations including and not including standing genetic variation.

Parameters: $s_1 = 0.05, s_2 = 0.05, \mu_1 = 10^{-5}, \mu_2 = 10^{-5}, N_{SDC1} = 10^5 - N_{SAN}, N_{SDC2} = 0$ cells, $N_{DDC} = 10^7$ cells.

Figure 4

We assume that there is an additional single-drug compartment where only drug 2 is active. We simulate the infection until there is colonization of the double-drug compartment and study the dependency of the relative frequency of the paths for stepwise resistance evolution on the compartment sizes, the mutation rates and the mutation costs. We consider the paths where only one of the single-drug compartments is colonized before treatment fails. Each point corresponds to the total fraction of patients that failed via the path *SAN* $\rightarrow$ *SDC1* $\rightarrow$ *DDC* relative to the total fraction that failed via the path *SAN* $\rightarrow$ *SDC2* $\rightarrow$ *DDC* out of 6000 replicates.

Figure 4a

We study the effect of asymmetrical compartment sizes on the stepwise paths to resistance evolution by increasing N_{SDC1} along the x-axis while keeping N_{SDC2} constant.

Parameters: $s_1 = 0.05, s_2 = 0.05, \mu_1 = 10^{-5}, \mu_2 = 10^{-5}, N_{SAN} = 10^5$ cells, $N_{SDC2} = 10^4$ cells, $N_{DDC} = 10^7$ cells.

Figure 4b

We study the effect of asymmetrical mutation rates on the stepwise paths to resistance evolution by increasing μ_1 along the x-axis while keeping μ_2 constant.

Parameters: $s_1 = 0.05, s_2 = 0.05, \mu_2 = 10^{-5}, N_{SAN} = 10^5$ cells, $N_{SDC1} = 10^4$ cells, $N_{SDC2} = 10^4$ cells, $N_{DDC} = 10^7$ cells.

Figures 4c

We study the effect of asymmetrical costs of resistance mutations on the stepwise paths to resistance evolution by increasing s_1 along the x-axis while keeping s_2 constant.

Parameters: $s_2 = 0.05, \mu_1 = 10^{-5}, \mu_2 = 10^{-5}, N_{SAN} = 10^5$ cells, $N_{SDC1} = 10^4$ cells, $N_{SDC2} = 10^4$ cells, $N_{DDC} = 10^7$ cells.

Part IV
Supplementary Figures

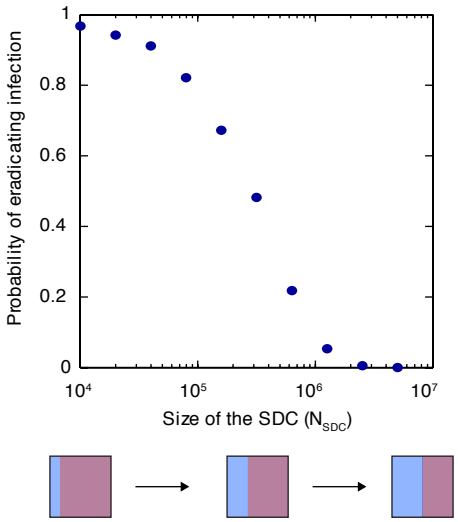

Figure 1: Eradication of an acute disease in the presence of single-drug compartments. The probability that a disease with no sanctuary is eradicated after treatment is plotted as a function of the size of the single-drug compartment with drug 1 (N_{SDC1}), assuming that the sum of the sizes of the SDC1 and the double-drug compartment is constant. Diagrams below the x-axis illustrate the changes in compartment sizes, following the style of Figure 1. The infection is simulated for 100 days before treatment. Treatment starts after this time and is simulated until there are no infected cells in the body (disease eradication) or until the double-drug compartment is colonized. Parameters: $R_{WT} = 4, \epsilon_1 = 0.99, \epsilon_2 = 0.99, d_y = 1\ \text{d}^{-1}, d_x = 0.1\ \text{d}^{-1}, m = 0.1\ \text{d}^{-1}, s_1 = 0.05, s_2 = 0.05, \mu_1 = 10^{-5}, \mu_2 = 10^{-5}, N_{SAN} = 0$ cells, $N_{SDC2} = 0$ cells, $N_{DDC} = 10^7 - N_{SDC1}$. N_{SDC1} changes along the x-axis. Each point corresponds to 3000 simulated patients.

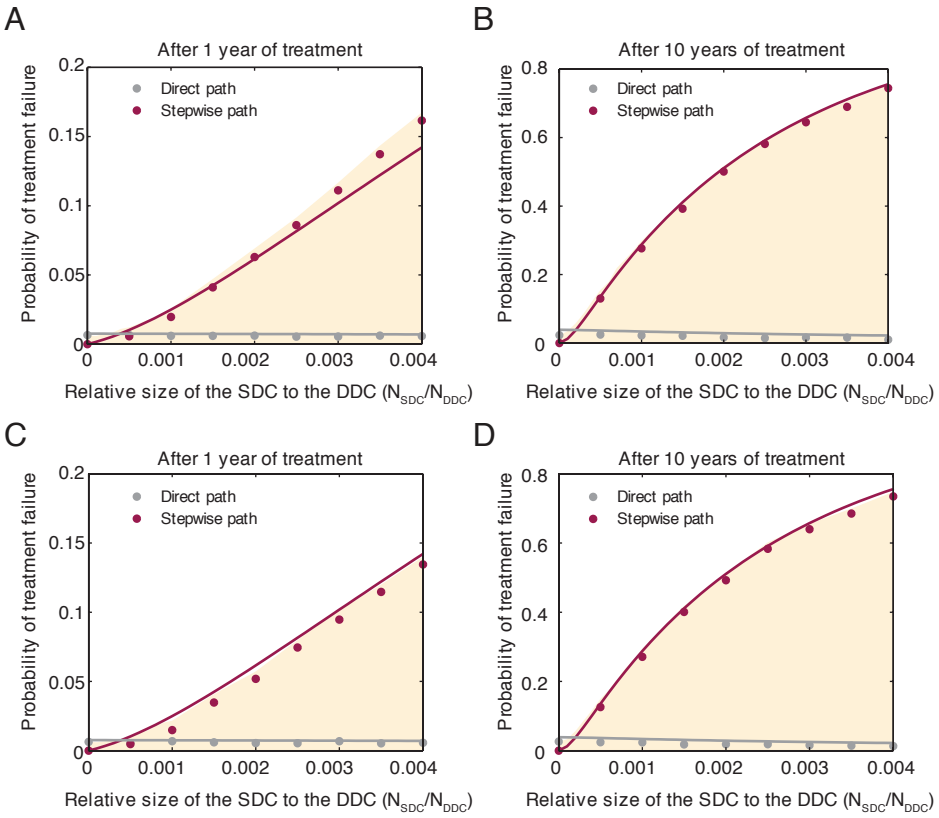

Figure 2: Resistance evolution in the presence of single-drug compartments and pre-existing resistance. (A and B) The shaded area gives the fraction of simulated patients that failed treatment after 1 or 10 years as a function of the size of the single-drug compartment containing drug 1 (SDC1) relative to the size of the double-drug compartment (DDC). The infection in all the compartments is simulated for 100 days before treatment starts. We further indicate whether treatment failure occurred via direct (grey dots) or stepwise evolution (pink dots). Solid lines are analytic calculations (Suppl. Methods §5, 6). (C and D) Same as above, except that backwards migration is not allowed before treatment starts so the number of pre-existing mutants in the single-drug compartment corresponds to the expectation at mutation-selection balance and is not higher because of migration from the double-drug compartment as in A and B. Parameters: $R_{WT} = 4, \epsilon_1 = 0.99, \epsilon_2 = 0.99, d_y = 1\ \mathrm{d}^{-1}, d_x = 0.1\ \mathrm{d}^{-1}, m = 0.1\ \mathrm{d}^{-1}, s_1 = 0.05, s_2 = 0.05, \mu_1 = 10^{-5}, \mu_2 = 10^{-5}, N_{SAN} = 10^5$ cells, $N_{SDC2} = 0$ cells, $N_{DDC} = 10^7$ cells. N_{SDC1} changes along the x-axis for all the figures. For each value of N_{SDC1} treatment has failed in at least 300 simulated patients.

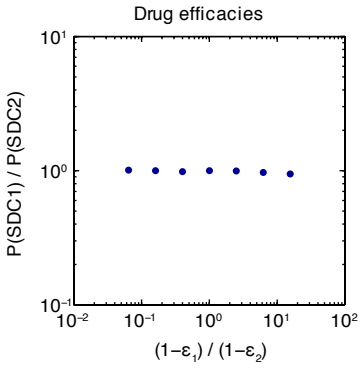

Figure 3: Stepwise resistance evolution in the presence of two single-drug compartments when drug efficacies differ. Fraction of simulated patients that failed via the path where the single-drug compartment with drug 1 is colonized before treatment failure (P(SDC1): *SAN* $\rightarrow$ *SDC1* $\rightarrow$ *DDC*) relative to the fraction that failed via the path where the single-drug compartment with drug 2 is colonized before (P(SDC2): *SAN* $\rightarrow$ *SDC2* $\rightarrow$ *DDC*) as a function of drug efficacies. The x-axis corresponds to the ratio of pathogen fitness in the presence of drug 1 relative to in the presence of drug 2, which is equal to one minus the efficacy of drug 1 (1-ϵ_1) over one minus the efficacy of drug 2 (1-ϵ_2). Parameters: $R_{WT} = 4, d_y = 1$ d$^{-1}, d_x = 0.1$ d$^{-1}, m = 0.1$ d$^{-1}, s_1 = 0.05, s_2 = 0.05, \mu_1 = 10^{-5}, \mu_2 = 10^{-5}, N_{SAN} = 10^5$ cells, $N_{SDC1} = 10^4$ cells, $N_{SDC2} = 10^4$ cells, $N_{DDC} = 10^7$ cells. The total number of simulated patients for each point is 10000.

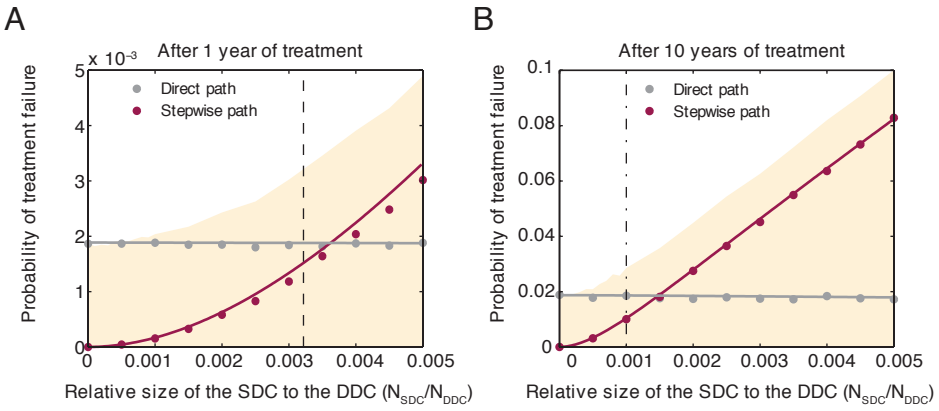

Figure 4: Resistance evolution in the presence of single-drug compartments in a region of the parameter space where the simplified Markov process has a good agreement with the stochastic simulations. The shaded area gives the fraction of simulated patients that failed treatment after 1 or 10 years as a function of the size of the single-drug compartment containing drug 1 (SDC1) relative to the size of the double-drug compartment (DDC). We further indicate whether treatment failure occurred via direct (grey dots) or stepwise evolution (pink dots). Solid lines are simplified analytic calculations (Suppl. Methods §5). The vertical dotted lines are analytical approximations for the point where the stepwise path to resistance becomes more important than the direct path (Supp. Methods §7). Parameters: $R_{WT} = 4, d_y = 1$ d$^{-1}, d_x = 0.1$ d$^{-1}, m = 10^{-3}$ d$^{-1}, s_1 = 0.1, s_2 = 0.1, \mu_1 = 10^{-4}, \mu_2 = 10^{-4}, N_{SAN} = 10^5$ cells, $N_{DDC} = 10^7$ cells. For each value of N_{SDC1} treatment has failed in at least 1000 simulated patients.

References

[1] Nowak, M. A. & May, R. M. C. *Virus dynamics: mathematical principles of immunology and virology*. Oxford University Press, USA, (2000).

[2] Perelson, A. S., Neumann, A. U., Markowitz, M., Leonard, J. M., & Ho, D. D. HIV-1 dynamics in vivo: virion clearance rate, infected cell life-span, and viral generation time. *Science (New York, N.Y.)* **271**(5255), 1582–1586, March (1996).

[3] Iwasa, Y., Michor, F., & Nowak, M. A. Evolutionary dynamics of invasion and escape. *Journal of Theoretical Biology* **226**(2), 205–214, January (2004).

[4] Haeno, H. & Iwasa, Y. Probability of resistance evolution for exponentially growing virus in the host. *Journal of Theoretical Biology* **246**(2), 323–331, May (2007).

[5] Hill, A. L., Rosenbloom, D. I. S., Fu, F., Nowak, M. A., & Siliciano, R. F. Predicting the outcomes of treatment to eradicate the latent reservoir for HIV-1. *Proceedings of the National Academy of Sciences* **111**(37), 13475–13480, September (2014).

[6] Pearson, J. E., Krapivsky, P., & Perelson, A. S. Stochastic theory of early viral infection: Continuous versus burst production of virions. *PLoS Comput Biol* **7**(2), e1001058, February (2011).

[7] Rouzine, I. M., Razooky, B. S., & Weinberger, L. S. Stochastic variability in HIV affects viral eradication. *Proceedings of the National Academy of Sciences* **111**(37), 13251–13252, September (2014).

[8] Karlin, S. & Taylor, H. M. *A First Course in Stochastic Processes, Second Edition*. Academic Press, New York, 2 edition edition, , April (1975).

[9] Alexander, H. K. & Bonhoeffer, S. Pre-existence and emergence of drug resistance in a generalized model of intra-host viral dynamics. *Epidemics* **4**(4), 187–202, December (2012).

[10] Kendall, D. G. Stochastic processes and population growth. *Journal of the Royal Statistical Society. Series B (Methodological)* **11**(2), 230–282, January (1949).

[11] Weissman, D. B., Desai, M. M., Fisher, D. S., & Feldman, M. W. The rate at which asexual populations cross fitness valleys. *Theoretical Population Biology* **75**(4), 286–300, June (2009).

[12] Hermisson, J. & Pennings, P. S. Soft sweeps molecular population genetics of adaptation from standing genetic variation. *Genetics* **169**(4), 2335–2352, April (2005).

[13] Bonhoeffer, S. & Nowak, M. A. Pre-existence and emergence of drug resistance in HIV-1 infection. *Proceedings of the Royal Society B: Biological Sciences* **264**(1382), 631–637 (1997).